CHARACTERIZATION AND MODELING OF DAMAGE IN STEEL AT DIFFERENT STRAIN RATES

A THESIS IN CIVIL ENGINEERING

Presented to the faculty of the American University of Sharjah
College of Engineering
in partial fulfillment of
the requirements for the degree

MASTER OF SCIENCE

by
REEM AL-HIMAIREE
B.S. 2009

Sharjah, UAE
January 2011

CHARACTERIZATION AND MODELING OF DAMAGE IN STEEL AT DIFFERENT STRAIN RATES

Reem Majeed Al-Himairee, Candidate for the Master of Science in Civil Engineering

American University of Sharjah, 2011

ABSTRACT

The structural behavior of steel, as many structural materials, changes during deformation processes under complex mechanical loadings. The damage process may start at some point in the deformation process in the form of micro-cracks and micro-voids leading at its latest stage to the development of macro-cracks and consequently material failure. Therefore, systematic understanding of the ductile failure mechanism due to accumulation of plastic deformation is needed to enable proper structural design and hence provide better serviceability.

In the last two decades, the micro-structural concepts to define material failure have received wide attention as a better alternative to classical mechanics methodologies. The main objective of this research is to better understand damage initiation and evolution throughout the deformation process at different strain rates. The proposed study relies on a continuum damage mechanics approach that involves characteristic parameters to describe the accumulation of plastic strain and damage under different strain rates. The work has been divided into experimental, theoretical, and simulation phases. The experimental phase involves testing under monotonic uniaxial tensile loading to evaluate the tensile ductile damage behavior. The obtained material parameters are then used as the basic data in the simulations that are performed afterwards. Moreover, the damage is determined through two techniques: reduction in elastic modulus through loading-unloading curves and area measurements using Scanning Electron Microscope (SEM). The theoretical phase

proposes a new energy based model that captures the damage dissipation potential. The model has been confirmed theoretically by applying the proposed formula to the data available in the literature. Finally, this model has been implemented as a new user defined material in the finite element analysis software ABAQUS where damage is quantified. The results from the experiments and the model are then compared. In this context, a new damage identification procedure is presented and different aspects of it are particularly addressed.

The results of this study show that a simpler model can be utilized for damage assessment in steel based on the following conclusions:

- The rate of loading is a main sensitive parameter that affects damage, as it has increased significantly with increasing loading rate. Towards higher loading rates, the damage grows in a faster mode.
- Damage is highly a nonlinear process indicating the steel is pushed closer to a complete state of fracture with the accumulation of strain.
- The comparisons indicate good agreement between the experimental and the applied energy based model results.
- The results using elastic energy equivalence yields more conservative values of damage than the strain equivalence hypothesis.
- The agreement between parameters that are measured by the new approach and those found in the literature are good.
- The finite element analysis has shown a good correlation with the model predictions.

CONTENTS

LIST OF ILLUSTRATIONS

LIST OF TABLES

ACKNOWLEDGEMENTS

First, I would like to thank Allah for paving me the way to reach this level of education and accomplish this work.

I would like to express my gratitude to my research advisors, Dr. Adil Al-Tamimi and Dr. Farid Abed, for their advice, encouragement and dedication. Their advanced expertise in materials and structures combined with a friendly personality made them great mentors throughout my graduate studies at AUS. I am also very thankful to the members of my committee, Dr. Jamal Abdullah and Dr. Nasser Qadoummi, for their valuable suggestions.

Special thanks to Mr. Arshi Faridi, Mr. Aqeel Ahmed, Mr. Recardo and Mr. Salman Pervaiz for their enthusiastic help and assistance during the testing stage of the project. I appreciate also the technical support of the Petroleum Institute in Abu Dhabi in particular Dr. Thomas Steuber and Ms. Melina Miralles. The challenging discussions we had there, made this academic experience very memorable.

I wish to thank my colleagues, friends, and the faculty and staff of the College of Engineering. Finally, saving the best for the last, I will be forever indebted to my family. Without their unyielding support, I would not be standing here. Thank you all.

To the person who was the wind beneath my wings

CHAPTER 1

INTRODUCTION

This chapter introduces the area of the continuum damage along with its relevant applications. It will address also the research motivation, potential application and challenges in the field of continuum damage. Finally, the objective of this thesis along with a general outline of the next chapters is provided.

1.1 Research Motivation

Steel products (chosen research material) have wide applications in aerospace, railways, mining, and automotive design. High quality steels are also used as a skeleton supporting many infrastructure constructions like, for example, skyscrapers, arenas, stadiums, bridges and others. In addition to their use in the construction of bridges, they are used in pressure vessels, storage tanks, etc [1].

Under applied loadings, structural/mechanical properties of steel (as other real life structural materials) change leading to material deterioration. Examples of these properties are strength, toughness, electrical resistivity and ductility. ASTM standards concerning structural design codes does not account for the change in material properties under different loading rates although the consideration of rate dependence on material behavior is quite important in structural design since material performance do change under different strain rates. For these reasons, the investigation of structural behavior over a wide range strain rates has been studied extensively in the last few decades, both experimentally and theoretically [2].

Additionally, the presence of damage also affects the material response due to the fact that it is related to the irreversible processes that takes place in the microstructure. Examples of conditions where plastic strain reversals may occur are earthquake loadings, cyclic overloads and the reeling of pipelines. Still little attention has been given to the possibility of incorporating damage into plasticity by means of micromechanics [3]. Many damage models have been proposed; however, the

initiation of ductile macro-cracks of metal under complex stress states could not be correctly predicted. Methodologies of classical fracture mechanics were successful in solving different types of problems but they still face many limitations. They fail to solve problems for finite strain plasticity, interactions of multiple types of damage, problems considering three dimensional effects, etc. A Continuum Damage Mechanics (CDM) approach was developed to resolve these problems. It develops quantitative relationships between atomistic, microscopic, and macroscopic parameters. The primary purpose of CDM is to describe the coupling effects between damage processes and the stress-strain behavior of materials. The main principle of CDM introduces a continuous damage variable which describes the intensity of the micro-defects in a structural material or component. When this variable reaches its critical state, macroscopic defects will be created leading to complete failure [4]. The choice of the damage parameters is a critical issue in CDM. These parameters should have clear physical, mathematical and mechanical properties to develop an efficient and accurate model. In addition, measuring these parameters that indicate material degradation in a reliable technique or instrument is still a challenging task. Also, the damage model should be easy to deal with and efficient numerically but at the same time it should not neglect any of the essential parameters [5].

Many researchers developed different models and characterizations that are difficult to compare with each other and sometimes end up with contradictory results (examples [6, 7]). Most of the methods involve intricate numerical analysis or huge experimental setup. Conducting such tests require high cost and time. First time users face many problems in using the literature for measuring or finding the damage parameters. Besides that, most of these models are difficult to incorporate in computer codes. Even the ones that are already built into commercial finite element codes, requires great experience and attention in order to avoid the danger of "numerical traps and tricks" [8]. It would therefore be of interest to have a simpler method for characterizing damage in these types of systems.

1.2 Related Applications

In recent years rapid advances have been made in materials technology, and the trend is set to continue. The use of modern materials encompasses all of the industries and has a strong influence on its competitiveness. However, to transform

these materials into competitive engineering products, the designer needs suitable design methodologies that satisfy material property requirements. The necessity for reliable data using validated measurement methods then becomes crucial. Furthermore, quantitative assessment of materials behavior and performance is essential to achieve quality and reliability of products [9].

Plastic deformation accumulation of metal is always a source of internal damage that leads ultimately to the failure or fracture of components/structures. As a result, it is crucial to understand the ductile damage of metal in large plastic deformation processes in order to improve product quality and process efficiency for engineering purposes. In this study, an experimental characterization of ductile isotropic damage evolution in steel is proposed to evaluate the essential damage parameters. The loading rates will be varied since they do affect the structural behavior of the material. This consideration is actually important in structural design and needs to be incorporated into standards and specifications.

Damage measurement emerges from many areas of applications. The most related application to the research area is the need to define damage for a specific engineering material and formulating the relevant equations for damage which are used to predict its evolution and the failure of the structure in service. In this way, an inclusive material description will be provided that involves not only the stress-strain response, but also the damage accumulation [1]. This will enable proper design of the structures to enhance safety, serviceability and manufacturing.

Damage phenomenon is “localized” in the material micro-scale and its effects remain restrained until the complete failure of several representative volume elements (discussed in more detail in Chapter 3) resulting in the formation of a macroscopic crack and hence failure of the structure/component as shown in Figure1 [10]. Of particular interest is how damage transfers from a lower scale to a higher scale. These micro-structural concepts will be utilized to assess the damage behavior in this work as the damaged surface will be observed in the Scanning Electron Microscopy (SEM), which provides real time monitoring of the damage process traced at the root of its occurrence. Sometimes engineers begin analysis with a macroscopic engineering model since it only needs macroscopically measurable properties, like hardness or elastic modulus that are relatively easier to handle [11].

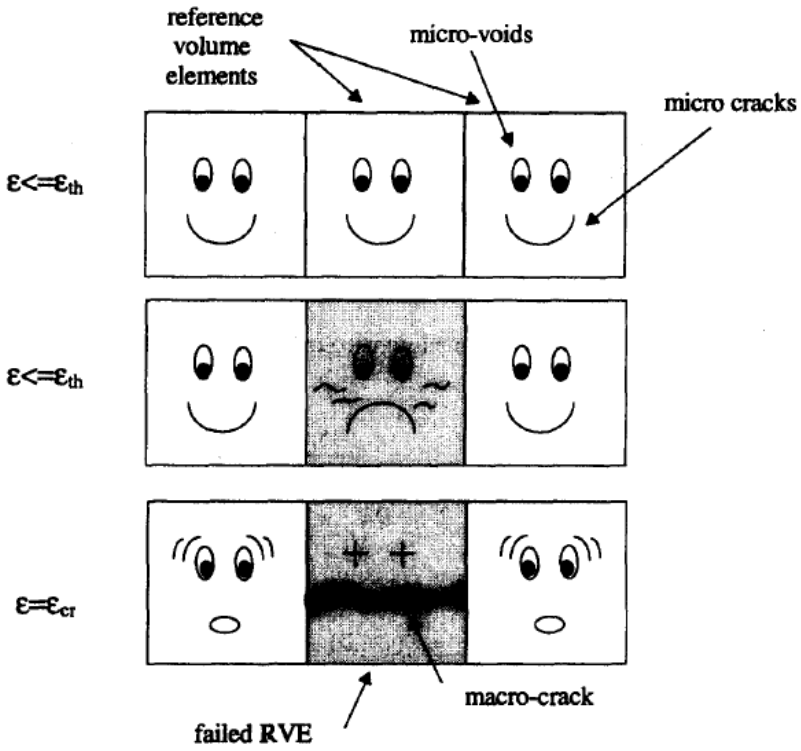

Figure 1. Sketch of the effect of localized damage on material macrostructure [10]

This work aims to develop a simple but powerful damage model to predict failure that can be used in the future to illustrate the influence of different loading regimes and to determine element failure in a finite element model. To accomplish this goal, experiments are performed on four series of specimens consisting of ten identical specimens in each series. The specimens are subjected to uniaxial monotonic loading with loading-unloading cycles. The damage is determined through measurements of the elastic modulus, Scanning Electron Microscope (SEM), and the newly proposed energy based model.

While the concept of ductile design is simple, its implementation is more complex, both at a design and a research level. The reported research aims to address a key question associated with ductile design, namely:

Can a simple model, to be developed in the future as a tool for finite element modeling (FEM), predict the failure of an element based on its strain history and maybe complement or even replace the need to evaluate failure based on full scale testing? The proposed technique in the next chapters offers a practical key to these questions.

1.3 Objectives

- To review some general features of CDM and to study its main aspects focusing on the definition and measurement of damage in order to be able to describe the mechanical behavior of the damaged material.
- To understand the damage mechanism in steel specimens under uniaxial tensile loadings at different strain rates.
- To represent a discontinuous state (micro-cracks and micro-voids) by a continuous variable φ that is determined by three methods compared to each other: the change of modulus of elasticity, the use of microscopy (SEM), and the utilization of energy principles.
- To develop a strain rate-dependent model for structural damage that takes account of plastic strain, loading rates and strength using the concepts of effective stress after obtaining and analyzing the results of the previously mentioned three techniques.
- To predict the failure in steel using the proposed damage model.
- To verify and compare the results using a finite element model.

1.4 Contribution to the State of the Art

The thesis in general contributes to the growing field of micro-structural modeling. Specific contributions of the thesis are mainly those addressing the challenge of developing a simple reliable damage model for ductile fracture based on continuum approach. Listed below are the detailed contributions:

- The continuum damage model introduces a damage variable which represents the deterioration of a material state before the initiation of macro-cracks. The assessment of this variable is often money and time consuming. This study proposes a model that evaluates the damage variable while providing cost and time saving.
- Accordingly, the damage approach developed here can provide a new method for both design of new structures and estimation of the remaining lifetime of existing structures under service loading conditions.
- The model discussed in this research can be implemented in a finite element code in the future in order to follow ductile crack growth. Alternatively, it can be used as a post-processor tool to calculate the time and location of a

macroscopic crack initiation in a structure or component under large plastic deformations.

1.5 Thesis Structure

Having introduced the topic in the first chapter, a literature review will follow to look at related work in this field in Chapter 2. This chapter will briefly review literature in terms of available damage models. Next Chapter 3 will explain continuum damage mechanics and in particular ductile damage. It also sets the base for the work done in this thesis. In Chapter 4, the experimental identification procedure is presented and discussed in detail along with material parameter evaluation criteria. The data and results are presented in Chapter 5 for all experimental, theoretical, and numerical approaches. Chapter 6 discusses and analyzes the results. It also includes comparisons with results from the literature. Finally, Chapter 7 concludes the work by a summary along with the limitations and directions for future research.

CHAPTER 2

LITERATURE REVIEW

Chapter 2 introduces the phenomenon of damage along with its associated variables. Most of the sections presented in this chapter are connected inherently to Continuum Damage Mechanics Modeling (CDM) approach (discussed in detail in the next chapter). The chapter ends with the literature survey summarizing research done in damage mechanics.

2.1 Damage

2.1.1 General Overview

Real life structural materials are exposed to different types of loadings leading to material deterioration and change in their structural/mechanical properties. This progressive physical process of degradation in the mechanical properties with complete loss of stress carrying capacity is commonly referred to as damage. Damage diminishes material strength, hardness, modulus of elasticity, density, and the yield stress. On the other hand, it enhances the creep strain rate and the electrical resistance.

Chaboche [12] shows that the phenomenon of damage is characterized by the initiation, coalescence and growth of micro-defects such as micro-voids and micro-cracks at any stress concentrators, which include inclusions, grain boundaries, and inhomogeneities, resulting in complete failure of the material as shown in Figure 2. Lemaitre and Dufailly [5] identified these micro-defects or discontinuities in solid materials as micro-cracks or voids in metals, interface decohesions between cement, sand, and aggregates in concrete, and bonds breakage in polymers and composites. It is crucial to note that micro-cracks and voids do open under tensile loads and they close under compressive ones and thereby affecting macroscopic properties differently [11].

Damage in materials can be divided into several types according to the prevailing macroscopic behavior, as mentioned by [13], [14], and others in the literature. These types include brittle, ductile, creep and fatigue damages. In brittle

damage, micro-defects are initiated without significant plastic strains unlike ductile damage in which micro-defects are caused by large plastic strains. Creep damage is related to high temperature loadings while fatigue damage is formed due to cyclic loadings.

2.1.2 Damage Variable

A damage parameter φ is introduced, which represents the damage evolution. Voyiadjis and Kattan [4] defined the damage variable φ for the case of isotropic damage using the effective stress concept as the following:

$$\varphi = \frac{\mathbf{A}-\bar{\mathbf{A}}}{\mathbf{A}} \qquad \text{Eq. 1}$$

where $\bar{A}$ is the effective net area and A is the damaged area as shown in Figure 3. The net area can be calculated by subtracting the areas of the micro-defects. The previous expression shows that when φ=0, the material is undamaged (the damaged area and effective undamaged area are the same). On the other hand, when φ=1 the effective

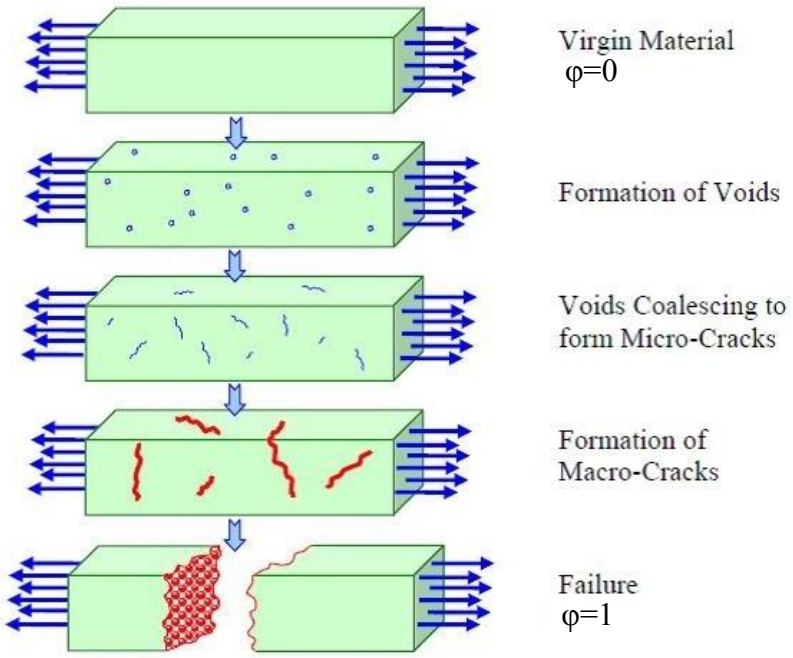

Figure 2. Damage in terms of crack evolution [15]

area is zero and material is totally damaged with a complete loss of material's structural integrity (i.e., fracture of the Representative Volume Element (RVE)), Figure 2. The theoretical value of φ is between $0 \leq \varphi \leq 1$ while in reality Lemaitre [16] set the critical value of the damage variable to be between $0.2 \leq \varphi_{cr} \leq 0.8$ for metals.

2.1.3 Mechanics of Damage

Different damage models have been proposed in the literature. Today, all of these formulations stream from two main branches: classical fracture mechanics and continuum damage mechanics. The first one considers the process of initiation and growth of micro-defects as a discontinuous phenomenon and it applies more global concepts like the strain energy release rate, contour integrals, and stress intensity factors. Although classical fracture mechanics tools were quite successful in analyzing fracture globally and predicting crack initiation and growth mechanism in two dimensional elasticity or small strain plasticity that involves only proportional loading paths, their implementation still face some limitations; these concepts cannot be used for more complex analysis systems including finite strain plasticity, ductile fracture due to large deformation, time dependent behavior, and three dimensional effects with loading paths not to be proportional [4]. On the other hand, in continuum damage mechanics the damage is assumed to be local and it introduces a continuous

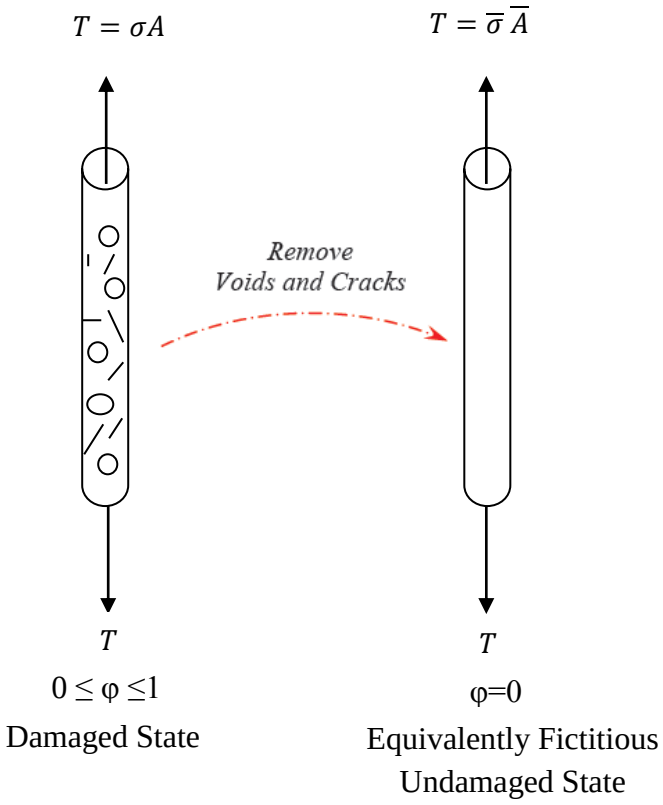

Figure 3. Damage in uniaxial tension (concept of effective stress) [6]

scalar damage variable in the process zone. The process zone in continuum damage mechanics is a zone that has reached critical damage conditions with high gradients of rigidity and strength, that is a crack. The micro-damage model is only material dependent, and not geometry dependent, which gives it a great advantage over conventional fracture mechanics. Moreover, the damage model allows damage measurement at every point of a structure for any geometry or loading, provided that the damage mechanisms and stress-strain curves are known [17]. Therefore, the development of micro-structural damage in engineering materials can be effectively modeled using continuum damage mechanics.

2.2 Related Work

In the last three decades, micromechanical modeling has been developed resulting from a deep understanding that the processes responsible for macroscopic failure are deeply rooted in the material microstructure. The process of material degradation due to nucleation and growth of defects, termed as damage, was first used to predict the creep rupture of metals in service at elevated temperatures by Kachanov [18].

Since the early work of Kachanov in 1958, the CDM framework for ductile damage was later developed mainly by Lemaitre and Chaboche. Following the same scheme, several damage models using special expressions for the damage dissipation potential have been proposed by different authors (Tai [19], Chandrakanth and Pandey [20], Bonora [21] and Zheng et al.[22]). However, in most cases these models were able to describe only damage evolution for particular metals and some of the model parameters did not have a clear physical meaning and identification procedure. Moreover, the arbitrary choice of the damage variable parameters led in many times to different and often contradictory models to be proposed see e.g. [6, 7].

Several models have been developed that account for both the damage and plastification phenomena as they occur simultaneously such as Voyiadjis and kattan [4] and LaEmmera and Tsakmakisa [24] and Lubarda and krajcinovic [25].

Because damage mechanics deals with damage in terms of continuum variable, it is particularly well suited to approach crack initiation. Within this context,

different damage definitions and related models have been proposed and used in the last decades such as Dhar [26], Thomson and Hancock [27] and Lin et al. [28].

Different studies discuss the validity of the assumption of damage isotropy. Damage is anisotropic in nature as proposed by Chaboche [29], Murakami [30], Cordebois and Sidoroff [31]. At the same time these authors and others have shown that the identification of the damage parameters becomes difficult (see for example [32-34]). However, assuming isotropic damage in many cases is not too far from reality, at least in the deformation range up to the maximum engineering stress, and it is widely employed in the literature due to its simplicity and efficiency.

CHAPTER 3

CONTINUUM DAMAGE MECHANICS MODELING

Continuum Damage Mechanics (CDM) approaches the failure process in a given material from a local point of view. This chapter will present the theory and derivations of damage based on the assumption of uniaxial tension and isotropic damage. Additionally, damage quantification techniques will be discussed thoroughly.

3.1 Brief History

Originally, the primary concept of the theory of continuum damage mechanics was initiated by Kachanov [18, 35]. Its main notion was to describe the state of material damage with distributed micro-defects as a function of suitable mechanical internal state variables in order to formulate equations that will predict the mechanical behavior of damaged materials. This notion was then developed by other researchers and extended to include ductile, brittle and fatigue failures. Those main researchers were Lemaitre and Chaboche in France, Krajcinovic in the United States, Hult in Sweden, Leckie in England and Murakami in Japan [36].

3.2 Principles of Continuum Damage

3.2.1 Representative Volume Element

As mentioned before, Continuum Damage Mechanics (CDM) approaches the failure process in a given material from a local point of view. The basic definition of damage expresses it as the "effective surface density of micro-cracks and cavities in any plane of a representative volume element," [4]. The damage discontinuities or micro-defects are much smaller than the size of the Representative Volume Element (RVE) and much larger than the atomic spacing (See Figure 4). Thus, the appropriate linear size of the RVE is in the range of 0.05 to 0.5 mm for metals, 0.1 to 1.0 mm for polymers, and 10 to 100 mm for concrete [11].

To clarify the analogy of the RVE, choose an arbitrary point x^{macro} in a volume element at the macro-scale level where the material is considered to be homogenous

as shown in Figure 5. The magnification of this point will show the microstructure of the element.

In a similar pattern to the determination and testing of material properties and behavior of the macroscopic material, the volume V at the microscopic level will be the representative volume element for the whole material. This representative volume V has to be of a size that is large enough to contain large number of defects and small enough to be considered as a point at the macro-scale in order to employ the mechanics of continuum damage [37]. In other words, the dimension of the representative volume element *d* has to be much larger than the characteristic length *l* of the micro-defects and smaller than the length of the macroscopic element *L*; satisfying this condition $l << d << L$, the volume V is defined as the Representative Volume Element (RVE).

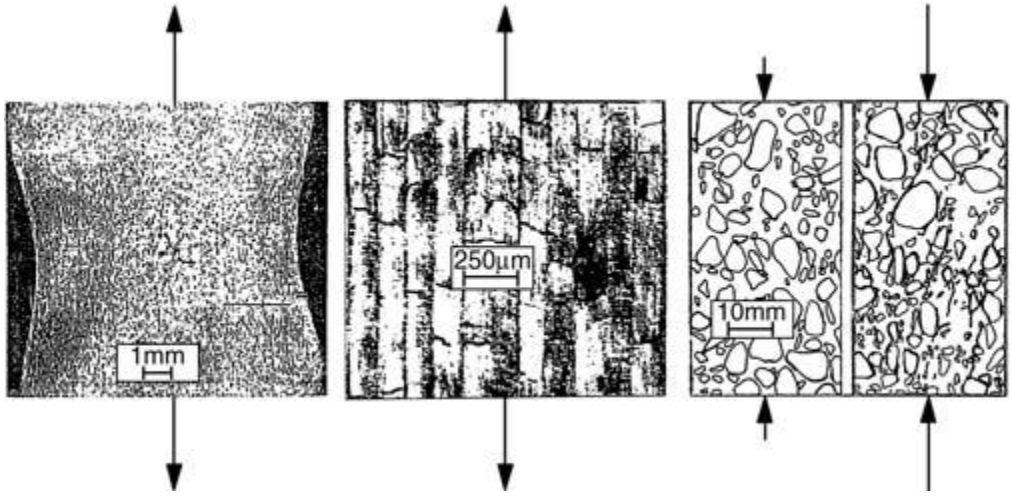

Figure 4. Examples of damage in a metal (left), in a composite (middle), and in concrete (right) [11]

3.2.2 Relations Between Damaged and Effective Configuration

The relations between damage and effective configurations are not yet fully defined. Two hypotheses are proposed in the literature: the hypothesis of strain equivalence and the hypothesis of elastic energy equivalence.

3.2.2.1 Equivalent Strain Hypothesis

It assumes the strain for both the damaged and the undamaged state is the same so that any strain behavior of a damaged material under the applied stress is equivalent to the strain of undamaged material under the effective stress [4].

3.2.2.2 Elastic Energy Equivalence Hypothesis

Sidoroff [32] identified the elastic energy equivalence hypothesis which states that "the elastic energy for a damaged material is equivalent in the form to that of the undamaged effective material."

3.3 Effective Stress and Effective Strain Concepts

If all types of damage, including voids and cracks, are removed from the RVE, one undamaged (effective) configuration is obtained, Figure 3. Since both configurations are subjected to the same external load T, then:

$$\boldsymbol{\sigma A = \overline{\sigma}\,\overline{A}} \qquad \text{Eq. 2}$$

The effective uniaxial stress can be found by substituting for the effective area from Eq.1:

$$\boldsymbol{\overline{\sigma} = \frac{\sigma}{1-\varphi}} \qquad \text{Eq. 3}$$

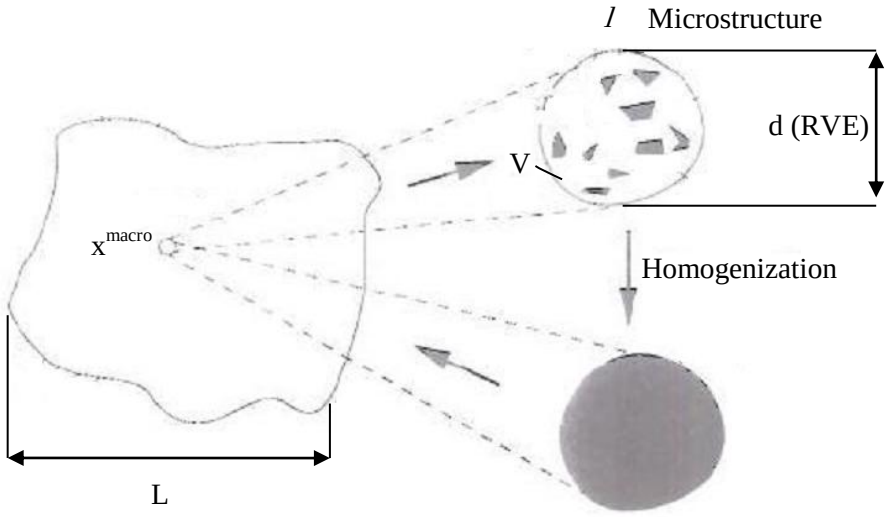

Figure 5. Representaive volume element characterization [37]

As mentioned before the derivation was made for uniaxial tension as shown in Figure 3, where the stress is obtained from Hooke's law of linear elasticity

$$\boldsymbol{\sigma = E\varepsilon} \qquad \text{Eq. 4}$$

where ε is the strain and E is the modulus of elasticity (Young's Modulus). Replacing the stress by effective stress, gives:

$$\boldsymbol{\overline{\sigma} = \overline{E}\overline{\varepsilon}} \qquad \text{Eq. 5}$$

The elastic strain energy scalar function U is defined as:

$$\boldsymbol{U = \frac{1}{2}\sigma\varepsilon} \qquad \text{Eq. 6}$$

Substituting for the stresses in the elastic strain energy equations for the damaged and undamaged states, the following relation is obtained:

$$\boldsymbol{\overline{\varepsilon} = (1 - \varphi)\varepsilon} \qquad \text{Eq. 7}$$

Substituting again equations 3 and 7 in 5 and simplifying the results and maintaining 4 in the right side, the modulus of elasticity is found to be:

$$\boldsymbol{E = \overline{E}(1 - \varphi)^2} \qquad \text{Eq. 8}$$

Finally, solving for the damage variable φ:

$$\boldsymbol{\varphi = 1 - \sqrt{\frac{E}{\overline{E}}}} \qquad \text{Eq. 9}$$

If we are to assume the hypothesis of strain equivalence where the strain and the effective strain are equal, the damage variable will be equal to:

$$\varphi = 1 - \frac{E}{\overline{E}} \qquad \text{Eq. 10}$$

where E is Young's Modulus of the damaged material and $\overline{E}$ is the effective undamaged modulus of elasticity as shown in Figure 6.

3.4 Isotropic Damage Evolution

During a deformation process the micro-defects may grow in certain directions depending on the stress distribution. The damage in this case is anisotropic and the

damage variable will be a tensor that is dependent on a unit normal vector on the plane of the representative volume element. However, if the growth of micro-defects is in one direction, then the damage is said to be isotropic and the damage variable will be a scalar [37]. In other words, it is assumed that the cracks and micro-voids are equally distributed in all directions. In the case of isotropic damage, the equations of evolution are easy to handle and it promises to assure adequate predictions of the load carrying capacity in structural components. On the other hand, anisotropic damage development has been studied by many researchers theoretically and proved empirically even if the virgin material is isotropic [4]. The same basic concept of progressive damage modeling is applied to both isotropic and anisotropic materials.

3.5 Damage Quantification

There are many ways to measure degradation in materials. Lemaitre and Dufailly [5] explained eight different experimental methods (direct and indirect) to measure damage based on the effective stress concept. The direct measurements include the observation of micrographic pictures using digital microscopes to measure the areas of cracks and the density variation measurement. The non direct destructive measurements are measurement of change in the elastic modulus, ultrasonic waves propagation and the non direct non destructive methods are the hardness variation measurement and the electric potential.

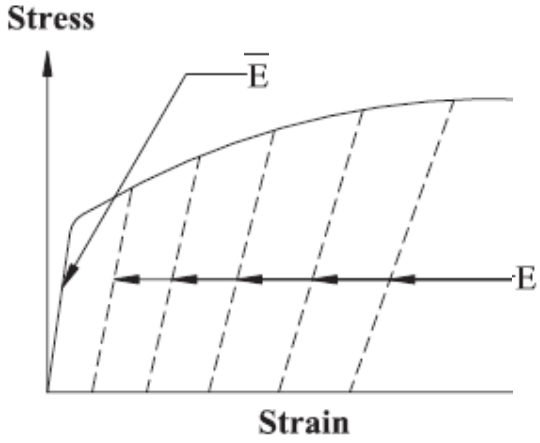

Figure 6. Modulus of elasticity for loading and unloading [16]

3.5.1 Direct Methods

They intend to quantify damage using pure geometrical considerations such as measurement of area fraction and density variation. Examples of previous work exploring these methods are [5, 26, 38-40]. Although these methods are used widely in the literature, their evaluation of ductile damage is still questionable due to the associated intrinsic experimental errors.

3.5.1.1 Measurement of Crack Areas

As suggested by Lemaitre [11], the first way to measure damage is to find the fraction area of voids at different plastic strain levels since the original definition of damage is related to the initiation and growth of micro-voids and micro-cracks; however, surface area fraction measurements suffer from errors depending on the equipment accuracy and the required specimen preparation. The tools of modern image analysis have significantly enhanced the use of this approach. For example, by using the scanning electron microscope and X-ray analysis for metals, specimen preparation is not required but limitations exist on the specimen dimensions, which will lead to other considerations during sample preparation in order to avoid introducing new damage or loss of apparent damage matrix during polishing. Additionally, knowing that the voids are smaller than few micrometers, variations in image magnification will play an important role in determining the void areas [41]. Lemaitre and Dufailly [5] specifies the appropriate magnification of the RVE as 1000X for metals and 10X for concrete in order to observe a picture of 100 X 100 mm in size. To reduce the effect of magnification on the accuracy of the results, [39] suggests taking pictures of different magnification in the range of 500-2000 times and measuring the area of micro-defects (A_{d1}, A_{d2} …A_{dn}) for n pictures with the area of every picture as S. The damage variable can be obtained using the following expression:

$$\boldsymbol{\varphi} = \frac{\mathbf{A_{d1} + A_{d2} + \cdots + A_{dn}}}{\mathbf{nS}} \qquad \text{Eq. 11}$$

Some of the published literature [43] utilizes advanced image analysis techniques from photo montages to image correlation techniques. A number of studies went to the extreme of examining the effect of the shape of the cavities on the damage parameter [44, 45].

3.5.1.2 Variation of Density

As mentioned by [46], density measurements resulted in significant disperses even with the use of high precision equipment. The expression of damage variable is shown below, where the density of the damaged state is ρ and $\bar{\rho}$ is the density of the initial (effective) undamaged state:

$$\varphi = \left(1 - \frac{\rho}{\bar{\rho}}\right)^{\frac{2}{3}} \quad \text{Eq. 12}$$

A critical assessment of damage evolution in different sheet metals was set by [46] using the indentation approach and compared to other experimental techniques (scanning electron microscopy, X-ray analysis and density measurements) and by finite element simulations.

3.5.2 Indirect Methods:

As an alternative to the geometrical methods, Lemaitre and Dufailly [5] qualify two indirect mechanical methods as the most promising methods for the determination of the damage parameter: determining ductile damage through its effect on the micro-hardness or the elastic modulus.

3.5.2.1 Variation of Elasticity Modulus

Damage in continuum damage mechanics (CDM) is an irreversible process that considers the degradation and loss of performance of materials resulting in stiffness reduction. Lemaitre [16] was the first to measure the damage variable through the degradation of the elastic modulus. From then on, determination of the elastic modulus was considered as the most reliable classical way of measuring damage. The damage variable can be found from analysis of loading and unloading curves using Eq.10, where E is Young's Modulus of the damaged material at any plastic strain and $\overline{E}$ is the effective undamaged modulus of elasticity:

$$\varphi = 1 - \frac{E}{\overline{E}} \quad \text{Eq. 10}$$

A study by [47] presented an experimental and numerical characterization of ductile damage evolution in steel subjected to large plastic deformations. Damage

evaluation was based only on measuring experimentally the Young's modulus for high levels of plastic deformation. The obtained factors are then used as the initial data in later simulations.

3.5.2.2 Variation of Micro-Hardness

Damage quantification based on hardness assumes that the hardness is linearly proportional to the flow stress. The damage parameter is determined through this formulation that was proposed by Lemaitre, where H is Vickers micro-hardness of the damaged material and $\overline{H}$ is the initial micro-hardness:

$$\varphi = 1 - \frac{H}{\overline{H}} \qquad \text{Eq.13}$$

The problem of the hardness technique is that it requires measurements of the micro-hardness along the axial length of the specimen along with curve extrapolation in order to determine the hardness in the virgin material, which cannot be measured directly [5].

Micro-hardness techniques have been used by [48] in order to determine damage parameters. Experiments were conducted by using a Vickers indenter in order to examine two types of steels and two aluminum alloys. The results showed that there is a good agreement between the measured values and the ones found in the literature. Some of the results drawn from the literature found that the micro-hardness technique is well suited to aluminum alloys but not for steels. This contradicts the study by [49] where good results were obtained in comparison to the change in the elastic modulus.

3.5.2.3 Variation of Electric Potential

Alternatively, it is also possible to evaluate damage using electric resistance techniques since the presence of voids affects the electrical resistance of metals. This has the advantage of being non-destructive and allowing for measurements to be made during deformation [50, 51]. However, it requires sensitive equipment and a sophisticated analysis of the data. The damage can be determined from the change in

the electrical potential, as in Eq.14, where V and $\overline{V}$ resemble the potential difference for the damaged and undamaged states, respectively:

$$\varphi = 1 - \frac{V}{\overline{V}} \qquad \text{Eq.14}$$

3.5.2.4 Ultrasonic Waves Propagation

This method requires the measurement of the propagation time of the waves. The degree of accuracy increases when the distance covered by the waves is large. This method is recommended for concrete with a frequency range of 0.1 to 1 MHz. For metals, this method is not adopted since the distance available for damage measurement is always small [5].

After the description of all methods, a damage definition is still somewhat difficult although many advanced technologies are being used such as acoustic emission, hydrogen absorption, and X-ray diffusion. The chart in Figure 7 was developed by [5] to aid in the method selection for each dominant phenomena as a function of the desired quality and the difficulty to evaluate.

Many researchers proposed different damage models that involved many parameters and conditions. A significant parameter to be considered during model development is the rate dependency, which was discussed in many publications. The effect of loading rate and fracture behavior of metal alloys were examined in [52]. Also, a rate dependent model for ductile damage was developed by [53], where the model has been verified numerically and using experimental data.

Some relevant studies to the research area are briefly; low-cycle fatigue damage micro-mechanisms was studied by [42] in a duplex stainless steel at room temperature using in situ microscopic device to follow the development and localization of the plastic slip markings. Qualitative and quantitative analysis on the micro-structural scale were performed using digital image correlation technique from surface images taken during cyclic loading. Another work was presented by [54], where a model was constructed to predict the onset of failure using finite element simulations and experimental results from the literature. The model was developed in ABAQUS using the user material option to describe ductile failure based on CDM approach.

Measurement	Brittle	Ductile	Creep	Low cycle Fatigue	High Cycle Fatigue
Micrography	*	**	**	*	*
Density		**	*	*	
Elasticity modulus	**	***	***	***	
Ultrasonic waves	***	**	**	*	*
Cyclic stress amplitude		*	*	**	*
Tertiary creep		*	***	*	
Micro-hardness	**	***	**	***	*
Electrical Resistance	*	**	**	*	*

three stars *** means “very good” two stars ** means “good”

one star * means “ try to see” no star means “ do not try”

Figure 7. Quality chart for methods of damage measurements [5]

CHAPTER 4

METHODOLOGY

The development of damage models was based on a program that consisted of experimental testing, theoretical work and finite element simulations. The objective of the experimental study was to identify the mechanical properties and characteristics of ductile damage in steel. Forty specimens were subjected to monotonic tensile loading under variable strain rates. The proposed energy model will be verified using previous publications. Additionally, Finite element simulations were performed in order to confirm the results of the new model.

4.1 Experimental Setup

4.1.1 Test Specimen

Round type specimens of length 200 mm and diameter of 12 mm were used in the tests. A sketch of the test specimens is shown in Figure 8. The experimental specimens were manufactured according to ASTM E9 standards [55] with the only modification of a shorter gauge length to enable the higher strain rates and prevent buckling due to high compression straining. The geometry of the chosen specimen has been widely employed in the literature due to the following main reasons; (1) pre-determined location of failure, (2) assumed proportional loading conditions along the minimum section; (3) the stress triaxiality is considered to be constant during the whole deformation process with the plastic strain as approximately uniform along the gauge length [56].

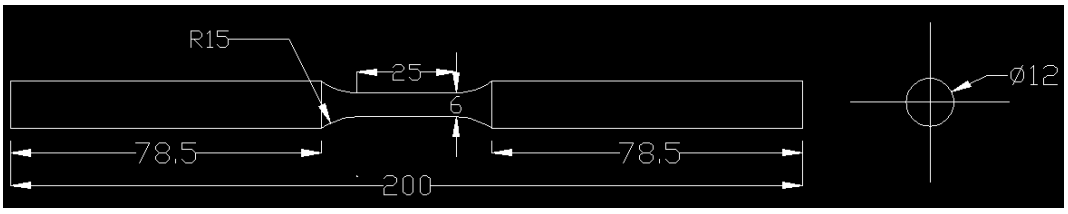

Figure 8. Geometry of the test specimen (dimensions in mm)

4.1.2 Material Specification

Grade 65ksi (448MPa) steel was used for the experiments. Table 1 shows the chemical composition of the structural steel used in the experiments. The measured yield and ultimate stresses of the material are around 460 MPa and 580 MPa, respectively. Other mechanical properties of the material extracted from tests are tabulated in Chapter 5.

Table 1: Chemical composition of grade 460 steel from supplier

Steel	C	Cu	Mn	Si	P	S	Ni	Cr
mass%	0.16	0.35	1.6	0.4	0.03	0.03	0.25	0.25

4.1.3 Instrumentation:

Universal Testing Machine (UTM) with 100 kN capacity was used to test the specimens in tension; Figure 9. Strain gauges with size of 5 mm were attached to the neck cross-section of the specimen using conductive adhesive; the strain gauge resistance was 120 X. The experiments were conducted at the room temperature (approximately 20˚ C). Crack measurements were performed using a Philips-FEI Quanta 200 SEM (available at Petroleum Geosciences department in Petroleum Institute, Abu Dhabi) equipped with an Energy Dispersive Spectrophotometer (EDS) that can image any sample without hiding any details or altering the composition. Figure 10 shows the adopted scanning electron microscopy.

4.2 Implemented Program

A total of 40 identical specimens were tested as classified in Table 2. A general description of the different stages follows. Detailed discussion of the results obtained in test series is presented in Chapters 5 and 6.

The experimental testing procedure is subdivided into the following steps:

STEP 1: Preparing the steel testing specimens according to ASTM E9 standards for testing with the help of the AUS Manufacturing Lab. A photo of the manufactured specimen is shown in Figure 11.

Figure 9. Photo of Universal Testing Machine Instron8801

STEP 2: Checking if the material satisfies the requirements for the proposed testing and model; it should behave in a ductile manner that allows for damage assessment at sufficient points with considerable difference in plastic strain.

Table 2: Distribution of specimens at different testing stages and loading conditions

Loading	Strain Rate1	Strain Rate2	Strain Rate3	Strain Rate4
At 0.1 Strain	SR1-0.1-1 SR1-0.1-2	SR2-0.1-1 SR2-0.1-2	SR3-0.1-1 SR3-0.1-2	SR4-0.1-1 SR4-0.1-2
At 0.15 Strain	SR1-0.15 -1 SR1-0.15 -2	SR2-0.15-1 SR2-0.15-2	SR3-0.15-1 SR3-0.15-2	SR4-0.15 -1 SR4-0.15-2
Near Ultimate 0.2 Strain	SR1-0.2 -1 SR1-0.2 -2	SR2-0.2 -1 SR2-0.2 -2	SR3-0.2-1 SR3-0.2 -2	SR4-0.2 -1 SR4-0.2-2
At 0.25 Strain	SR1-0.25 -1 SR1-0.25-2	SR2-0.25 -1 SR2-0.25-2	SR3-0.25-1 SR3-0.25-2	SR4-0.25 -1 SR4-0.25-2
Fracture	SR1-FR-1 SR1-FR-2	SR2-FR-1 SR2-FR-2	SR3-FR-1 SR3-FR-2	SR4-FR-1 SR4- FR-2

SR: Strain rate SR1=0.000333 s^{-1} SR2=0.00333 s^{-1} SR3=0.01 s^{-1} SR4=0.1 s^{-1}

Figure 10. Photo of Scanning Electron Microscope (Philips-FEI Quanta 200)

Figure 11. Photo of the manufactured steel specimen

STEP 3: Testing these specimens with varying loading rates according to the capability of the machine.

STEP 4: The specimens will be loaded and unloaded at different points on the stress-strain curve (in the hardening region before ultimate load, near the ultimate load, and after necking):

- Monotonic uniaxial tensile loading with displacement control (see Figure 12) was adopted using the Instron Universal Testing Machine (UTM) with a load capacity of 100 kN. The objective of using the monotonic test is to obtain the monotonic load-deformation characteristics.
- The total engineering strain was recorded by local strain gauges fixed at the gauge length. True strains were used for data analysis of large deformation systems by using the following equations, where ε_{tr} and ε_{eng} are true and engineering strains respectively and their corresponding stresses are σ_{tr} and σ_{eng} :

$$\varepsilon_{tr} = ln(1+\varepsilon_{eng}) \quad \text{Eq.15}$$

$$\sigma_{tr} = \sigma_{eng}(1+\varepsilon_{eng}) \quad \text{Eq.16}$$

- The rate of displacement used for the test is in the range of 0.5-150 mm/min.
- The loading-unloading series were carried out to measure the change in the elastic slope while the strain increased.

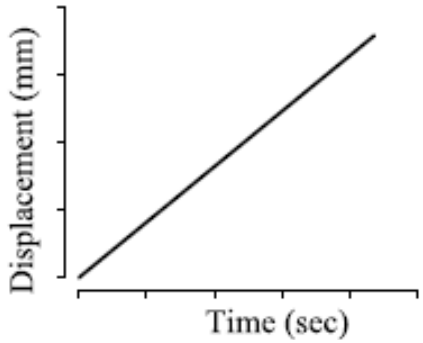

Figure 12. Loading path of the test [57]

STEP 5: After unloading, the specimen was cut to produce an image of the most damaged element using Scanning Electronic Microscope (SEM) to determine the void area fraction.

STEP 6: Evaluating the damage variable for each specimen using three approaches:

- Determination of the change in modulus of elasticity during unloading cycles. The damage variable will be obtained using the previously mentioned relations (Eq. 9 and Eq. 10) once assuming the elastic energy equivalence hypothesis and second assuming the hypothesis of strain equivalence, respectively:

  $\varphi = 1 - \sqrt{\frac{E}{\overline{E}}}$ and $\varphi = 1 - \frac{E}{\overline{E}}$

where E denotes the current unloading modulus and $\overline{E}$ is the effective undamaged modulus of elasticity as shown in Figure 13.

- Determining the effective areas using SEM images and then substituting it in the original definition of the damage variable, Eq.1:

$$\varphi=\frac{\mathbf{A}-\bar{\mathbf{A}}}{\mathbf{A}}$$

where $\bar{\mathbf{A}}$ is the effective net area and A is the damaged area. A reference specimen with no damage will be used first as a calibration measure. Here, the damage variable accounts not only for the effect of micro-defects but also for their mutual interactions.

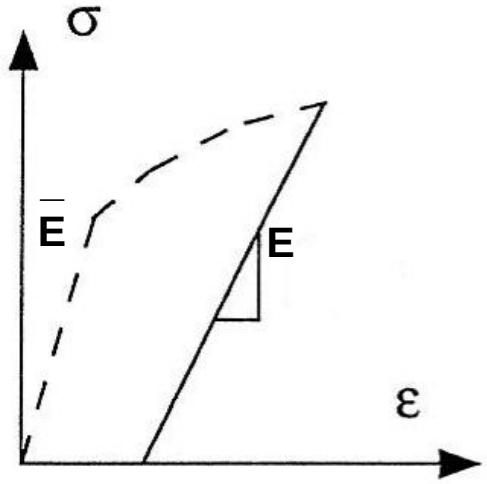

Figure 13. Example of experiment loading/unloading curve [11]

- Implementing energy principles by considering the stress-strain results of the tested samples as a measure of the materials capacity to accumulate damage. Once this capacity has been used up, the damage reaches 100% and failure will occur. The damage variable will be:

$$\varphi_p = \varphi_f \left(\frac{U_p}{U_T}\right)^{\alpha} \qquad \text{Eq.17}$$

where φ_f is the critical damage at failure, φ_p is the damage at any point during the deformation process and U_p is the corresponding energy at this point, U_T is the total energy and α gives the exponent of damage in relation to strain. The energy can be determined using the following expression, where σ and ε are true stresses and strains:

$$U = \int_0^{\varepsilon_p} \sigma \, d\varepsilon \qquad \text{Eq.18}$$

A theoretical verification of the method using previously published work will be presented in Chapter 5.

STEP 7: Verifying and comparing the results of the energy based model with a finite element model using ABAQUS software where the provided curves of damage development and true stress-strain are used as input for finite element calculations of the stress-strain behavior. This model can be used in the future for further analysis.

4.3 Material Parameter Identification

Development of damage models requires a precise control over the input variables and the measurement of a number of suitable response parameters depending on the failure mode. Following is a list of the measurements needed for development and evaluation of the damage models:

- The damage threshold strain ε_{th} is the strain value at which ductile damage will initiate. The exact determination of ε_{th} is difficult and for simplicity reasons, it can be considered the same as the strain corresponding to the proportional limit.
- The initial value of damage φ_o is very difficult to measure on a material for which the past loading history is unknown. It is related to the inclusions distribution in the virgin material. This parameter is often taken to be zero for a virgin material or at the beginning of the damage initiation. A scanning electron microscope investigation can give an idea of the initial amount of damage in a material by determining void fractions before loading.
- Critical damage variable, φ_{cr}. When this damage value is reached, failure occurs due to the reduced load carrying capacity of the effective net resisting area. Theoretically, the critical damage variable φ_{cr} is equal to 1 (complete fracture) while in reality experiments have shown that failure occurs much sooner than $\varphi = 1$ [58-60].
- The damage exponent α. This constant determines the shape of the law of damage evolution as a function of the accumulated plastic strain. Additionally, it takes into consideration the global effect of the void and crack growth stages on the damage development.

4.4 Model Assumptions

- The elastic deformations are assumed to be small relative to the plastic deformations.
- For the simulations, elastoplastic material behavior was assumed with Johnson-cook hardening.

4.5 Verification of the Optimum Method

One of the most important advantages of micromechanical models in comparison to other global approaches to fracture is that progressive damage can be modeled using material parameters only without referring to the geometry. This made the continuum damage approach as an optimum choice in this research and many others.

Different experimental procedures are used in the literature with variable definitions of the damage dissipation potential. The three methods for quantifying damage in this study were chosen by examining the previous publications and understanding the damage evolution process. Some of the suggested methods in the literature are not suitable for the present material. For example, the measure of damage using micro-hardness technique was suggested for aluminum alloys other than steel alloys.

Measuring damage through finding reductions in the elastic modulus for the material as a function of the applied strain is the most classical and reliable way of determining damage although it requires careful alignment of the sample and a sophisticated analysis of unloading and reloading curves [4, 16]. From here, the choice of this well-established technique was made.

The adoption of the fraction area of voids and cracks measurement method was due to the fact that the original definition of damage is related to the effective area concept. Modern image analysis tools have heightened the use of this approach to measure damaged areas. The Scanning Electron Microscope (SEM) is utilized in this study due to its great incorporated features. It produces easily interpreted micro-graphs and provides diverse information that can be employed for qualitative and quantitative analysis. The SEM is being used as a successful tool for material characterization since it reveals two or three dimensional information about the

microstructure, the chemistry, and crystallography of the tested material. SEM images have a large field depth that displays spatial variations, high quality of resolution and a wide range of magnification from 20X to almost 30000X. The SEM also can focus on specific points for analysis. SEMs are relatively easy to work with and they require few sample preparation steps. Generation of images takes time approximately less than five minutes. Additionally, these images can be converted to any suitable format. Some limitations include the sample size which can be a maximum of 10 cm horizontally and 40 mm vertically. SEM analysis does not lead to volume loss of the sample, so it is possible to analyze the same materials repeatedly [61].

The goal of this work was to examine the feasibility of developing a damage model that can be extended to different damage mechanisms and different materials. This simple model for characterizing damage employed energy principles. This model treats damage as an increase in the internal energy of the steel and consequently a reduction in its ability to absorb further energy prior to failure. Finally, data from previously published work and simulations of finite element were used to confirm the applicability of this model.

CHAPTER 5

DATA AND RESULTS

This chapter shows direct and indirect damage measurements as well as theoretical damage modeling. Direct measurements of damage was conducted using the scanning electron microscope, indirect damage measurements was obtained by considering the reduction in elastic modulus using loading-unloading curves, and finally a new energy model was proposed to predict the damage theoretically. Furthermore, the theoretical damage model was verified using finite element simulations and compared with the direct and indirect results of damage measurements.

5.1 Indirect Damage Measurements - Elastic Modulus Reduction

Damage effects are localized in the material microstructure as voids and cracks up to the appearance of a macroscopic crack. This localization can be experimentally quantified through the decrease of material stiffness. Tensile tests were conducted at room temperature at different strain rates with displacement-control mode (0.5–150 mm/min). The strain was measured with a small strain gauge positioned on the gauge length where plastic deformation starts to develop. The experimental engineering stress versus engineering strain data are shown in Figure14 for different strain rates. It can be seen that the yield stress changes significantly with the change in loading rates.

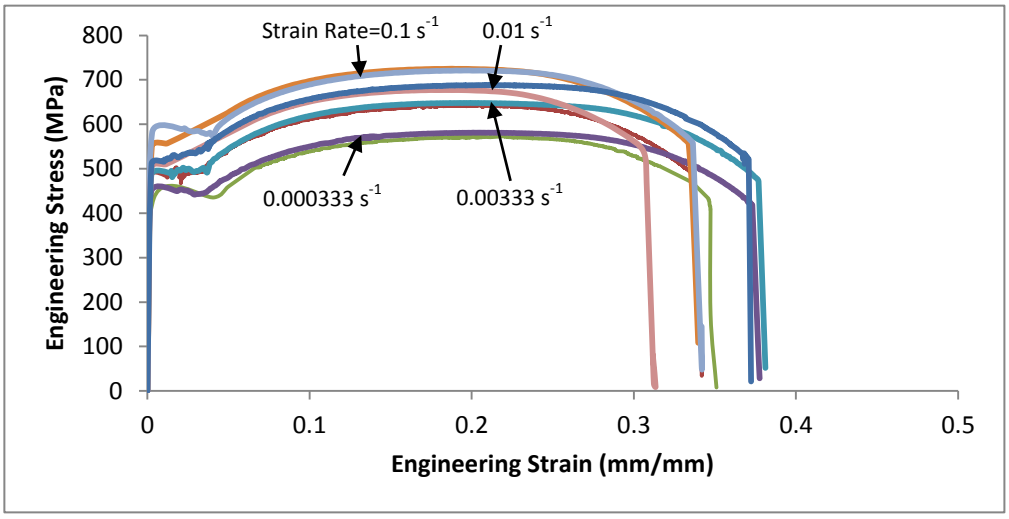

Figure 14. Stress-strain curves from uniaxial tensile test for steel at different strain rates

Damage measurement requires loading and unloading of the test specimen at different stages in order to determine the slope of the unloading curve which represents the elastic modulus of the damaged state. The damage variable is then computed using the elastic energy equivalence hypothesis and the hypothesis of strain equivalence, as defined by Eq.9 and Eq.10, respectively:

$$\varphi = 1 - \sqrt{\frac{E}{\overline{E}}} \quad \text{and} \quad \varphi = 1 - \frac{E}{\overline{E}} \qquad \text{Eqs.9 and 10}$$

where E denotes the current unloading modulus and $\overline{E}$ is the effective Young's modulus of the virgin material assumed to be 200 GPa for the studied material.

In this work, the specimens were loaded and unloaded at four engineering strains (0.1, 0.15, 0.2, and 0.25) in order to measure the decrease in the elastic modulus for varying strain rates. Sample graphs for all strain rates at 0.2 engineering strain are presented in Appendix. Two samples from each case were tested and the obtained values for the reduced elastic modulus were averaged. The systematic decrease in the elastic modulus at the chosen strains and strain rates is shown in Figure 15.

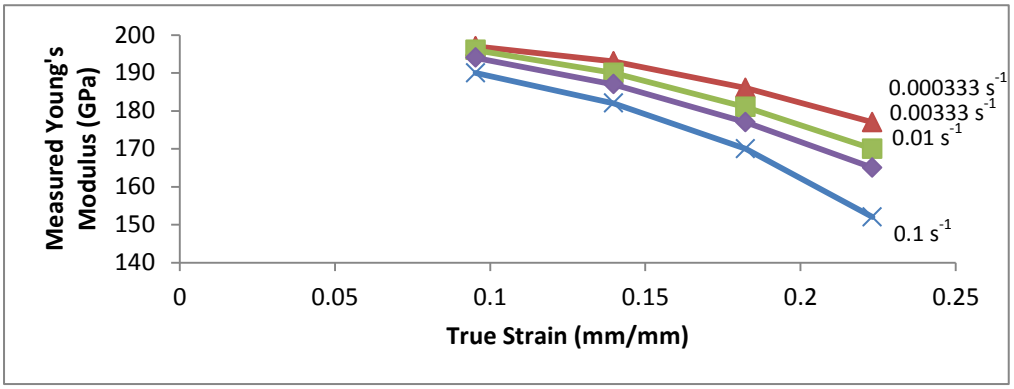

Figure 15. Experimental change of the elastic modulus with true strain at different strain rates

Substituting the values for the modulus of elasticity in the two different approaches Eqs.9 and 10 , the damage variable at different strain rates is calculated as depicted in Figures 16 (a and b). Towards higher strain rates, the damage increases in a faster manner. The observed trend shows that the difference between the damage obtained using the strain equivalence hypothesis and the one using the elastic energy equivalence hypothesis starts to increase with true strain for all strain rates; Figure 17 (a, b, c and d).

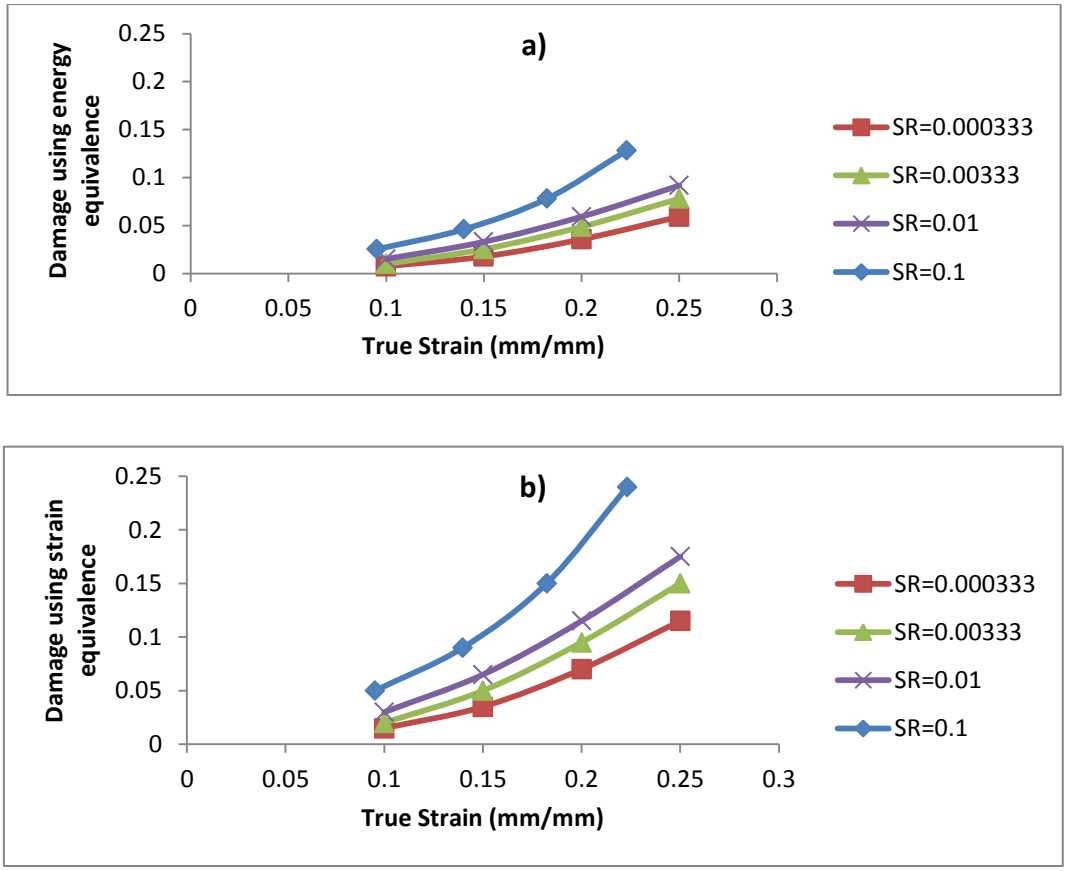

Figure 16. Damage vs. true strain for different strain rates using a) energy equivalence hypothesis and b) using strain equivalence hypothesis

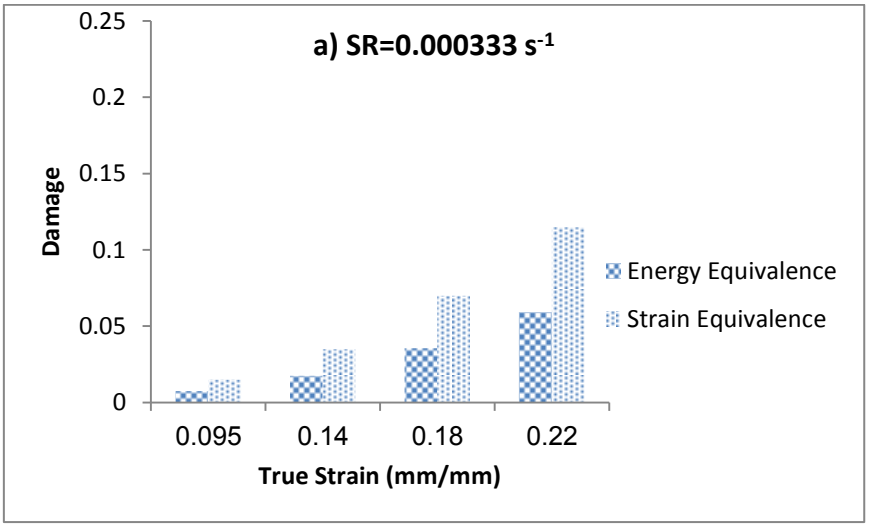

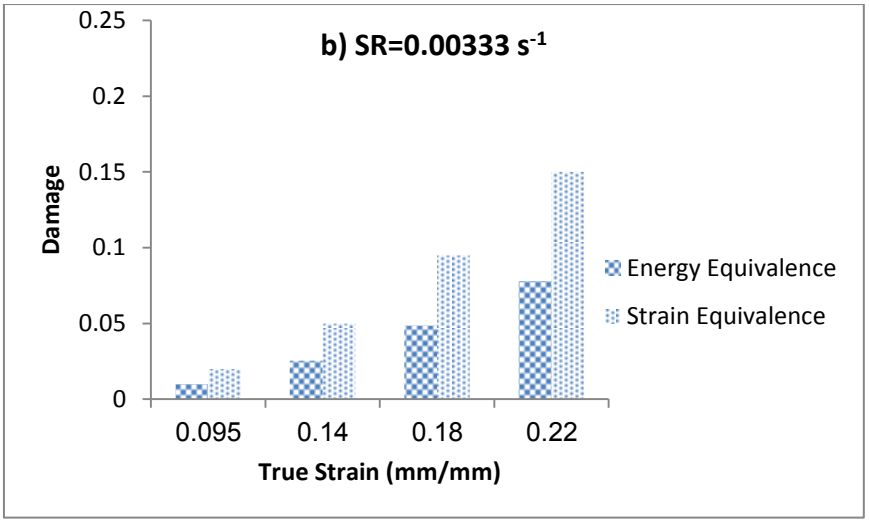

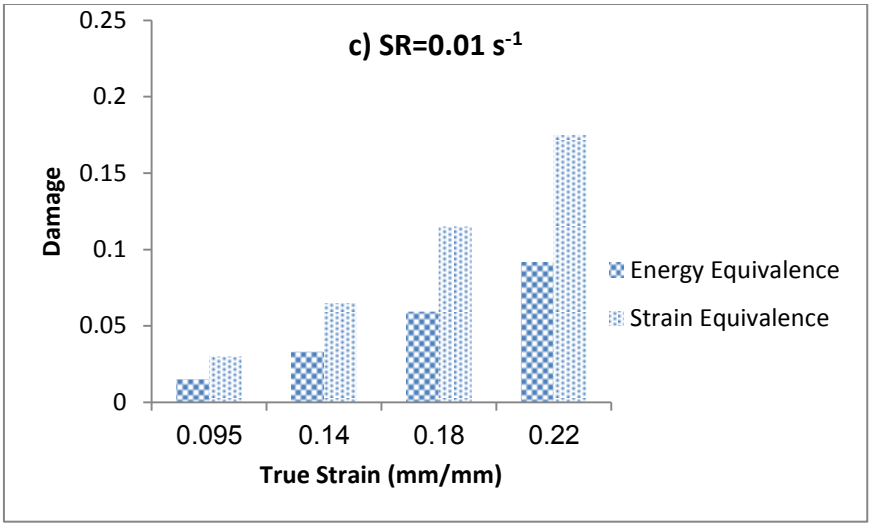

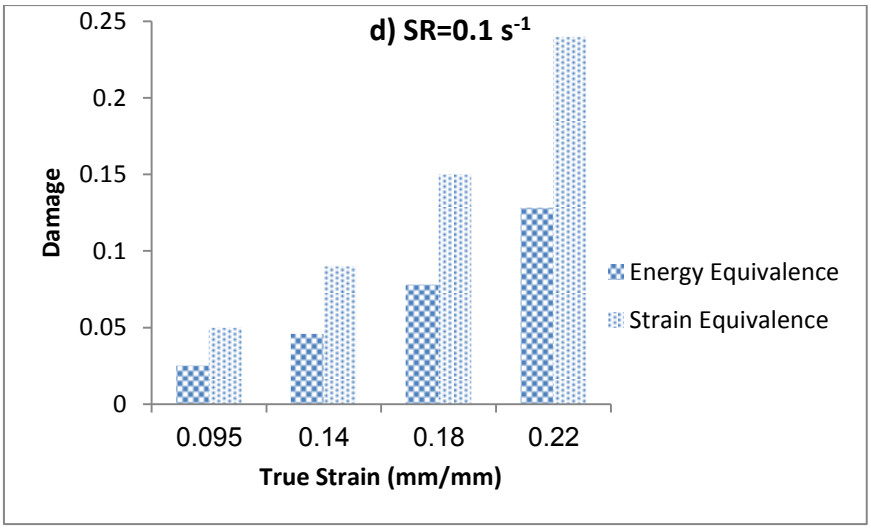

Figure 17. Damage using the elastic energy equivalence hypothesis and using hypothesis of strain equivalence for strain rate of a) 0.000333 s^{-1}, b) 0.000333 s^{-1}, c) 0.01 s^{-1}, d) 0.1 s^{-1}

5.2 Direct Damage Measurements - Scanning Electron Microscope (SEM)

As mentioned previously, the original definition of damage is related to the nucleation and growth of micro-voids and cracks. This section utilizes the effective area concept to measure the damage with the use of scanning electron microscopy that has significantly enhanced the ease of this approach.

Under different loading rates (0.5–150 mm/min), several specimens were loaded to different points on the stress-strain curve prior to fracture. After unloading the specimens, small (~ $2mm^3$) cylinders perpendicular to the tensile direction were cut out of the tensile test specimen at the necking area and then were slightly polished to reveal the micro-voids.

The Scanning Electron Microscope was used for image production and analysis and all void fraction measurements were performed on the surface area. The density of the micro-cracks in the RVE produced in the deformation process was taken as an index of damage. Images were obtained and the damage variable was found using, Eq.1. A reference specimen with no damage was used first as a calibration measure. Here, the damage variable accounts not only for the effect of micro-defects but also for their mutual interactions.

Damage is characterized by void nucleation, growth and coalescence and it is concentrated in regions near the fracture surface where plastic strains and the associated stresses are the highest. The void fractions were found using image processing techniques. The software that was used to handle images is called XL Docu. This program provides enhancements in image handling and manipulation, expanded measurement and annotation capabilities and flexible database image storage and retrieval. Thresholds were set to identify varying gray areas in the images to obtain binary images (Refer to Figure 18), such that everything below it in pixel numerical value is assumed to belong to an air void and everything above that threshold value is assumed to belong to solid surface. The ratio is then computed to obtain some kind of a density measure which could be highly correlated with the actual object density. Images at three magnifications (100X-1000X-2000X) were taken in which damage measurements showed very close results. Only results obtained from magnifications of 1000X were presented similar to [5]. At a

magnification of 50X, see Figure 19, the whole sample is shown but the micro voids are not visible. The initial void fraction for the present steel was found to be 0.0003~0. Figure 20 shows some of the obtained SEM micrographs of the microstructure with the strain rates and damage variables indicated. The damage variables versus the strain were plotted in Figure 21.

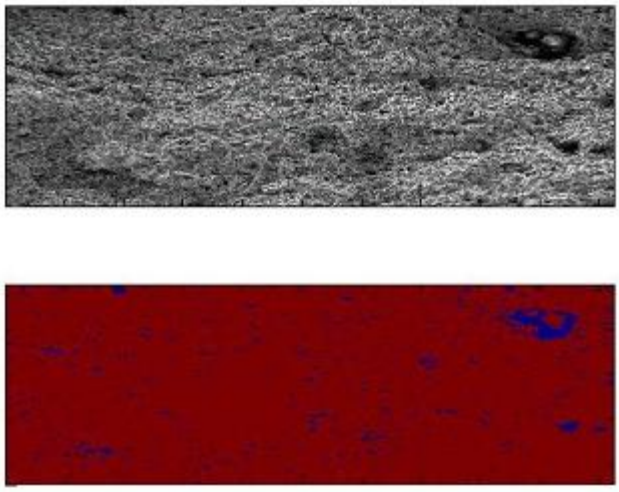

Figure 18. Image obtained from SEM and the corresponding binary image

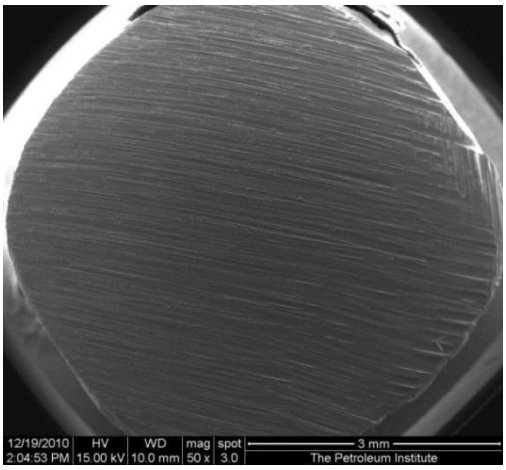

Figure 19. Representative cross-section area of a damaged specimen at magnification of 50X

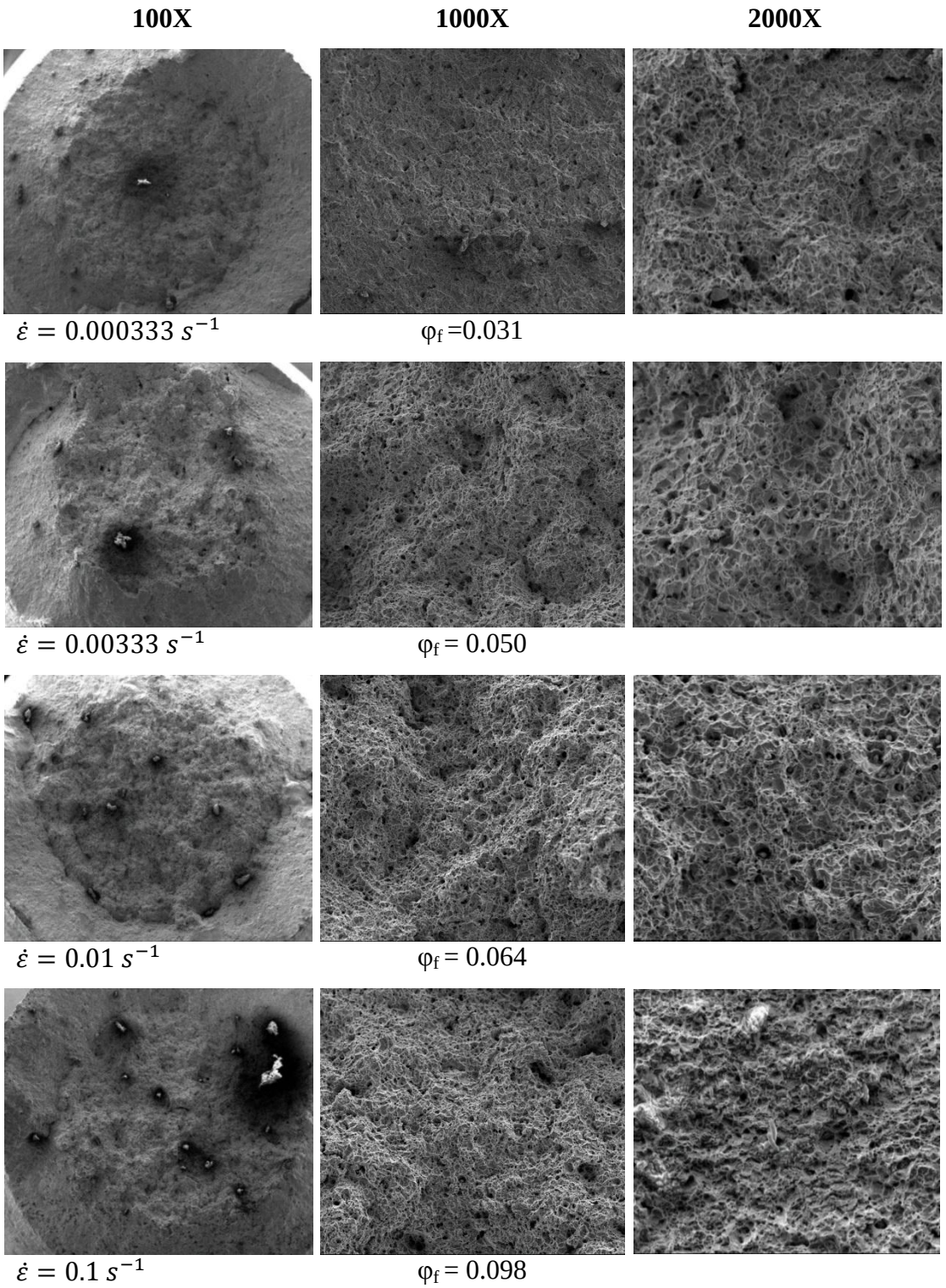

Figure 20. SEM images of fractured damaged surfaces at different strain rates

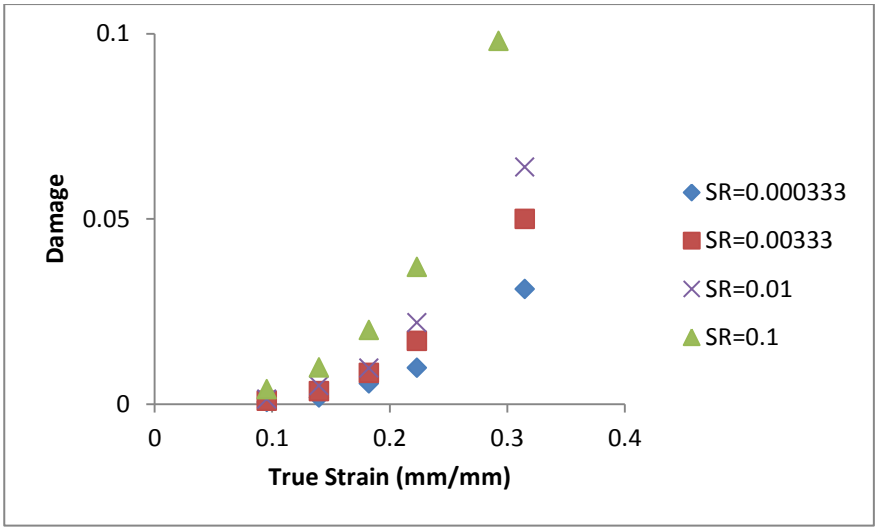

Figure 21. Damage vs. strain for different strain rates using SEM images

5.3 Theoretical Damage Modeling –Energy Concept

5.3.1 Model Implementation Results

The proposed energy based model considers the area under stress-strain curve as a measure of the materials capacity to accumulate damage. Once this capacity has been used up, the damage reaches 100% and failure will occur. This model is based on the hypothesis that damage dissipates nonlinearly as a function of the effective accumulated plastic strain and taking into account the global effect of nucleation, growth and coalescence of micro-voids in a ductile failure process. The damage variable is evaluated using Eq.17:

$$\varphi_p = \varphi_f \left(\frac{U_p}{U_T}\right)^{\alpha} \qquad \text{Eq.17}$$

where φ_f is the critical damage at failure, φ_p is the damage at any point during the deformation process and U_p is the corresponding energy at this point, $U_T$is the total energy and α gives the exponent of damage in relation to plastic strain. The energy can be determined using the following expression, where σ and ε are stresses and strains:

$$U = \int_0^{\varepsilon_p} \sigma \, d\varepsilon. \qquad \text{Eq.18}$$

The total energy at each strain was evaluated and the model parameter $\alpha = 2$ was identified using the experimental stress strain results. Figure 22 depicts the trends of damage variable throughout the sample deformation predicted using the proposed damage model. Results show almost identical curves for all of the four considered rates due to assumption of the damage at failure to be equal to unity for all strain rates.

5.3.2 Model Verification

5.3.2.1 Model Verification Using Literature

Continuum Damage Mechanics (CDM) has been widely applied in the modeling of the mechanical behavior of a damaged material that contains distributed defects. It introduces a state variable to describe the severity of damage and the evolution of the damage. This variable can be determined using different methods as discussed in Chapter 3. For the sake of verifying the validity of the proposed energy based model, input data were extracted from the literature and the energy model was implemented. The results of the literature were compared to the ones found from the model. The agreement between parameters that are measured by the new approach and those found in the literature are good. The examined literature cases differed in the assumption of whether the damage evolution is a linear process or not and thus varying the values for the constant α.

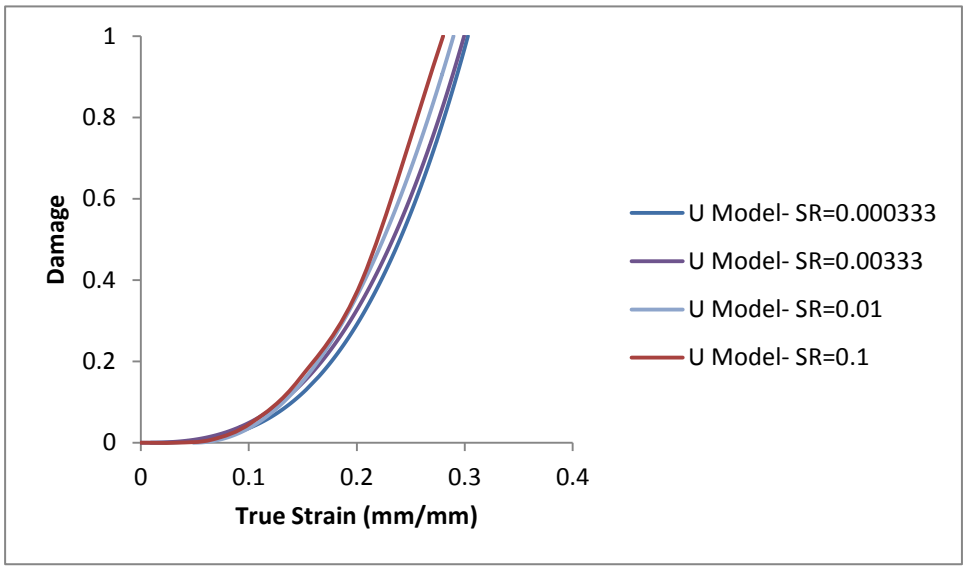

Figure 22. Damage values for different strain rates based on the proposed energy model

5.3.2.1.1 CASE 1: A New Procedure Using The Microhardness Technique for Sheet Material Damage Characterization [48].

The experimental characterization of damage was performed using micro-hardness techniques for different types of steel and aluminum alloys. The micro-hardness measurements were performed at the area where plastic strain was the highest. Damage evolution was provided for different materials. Results prove that the new procedure is satisfactory for damage characterization and offers some simplifications. The stress-strain curves of the materials and the identified damage are shown in Figure 23 and Figure 24, respectively. The data were tabulated using a software digitizer. Next, the hardening parameters were determined using a power curve fit in Microsoft Excel; Figure 25. The obtained equations were used to find the energy at every strain.

Reliability of the provided damage values was confirmed by [48] via comparing them with the literature information on HSLA steel and conventional steel XC60. The energy based model was applied with the constant α taken as 1 since the paper assumes that the damage correlates linearly with strain and the values used for φ_f were the ones found in the paper. The comparison between the two approaches is presented in Figure 26 for two steel types. In spite of the variation between results, it can be said that error may be considered relatively low.

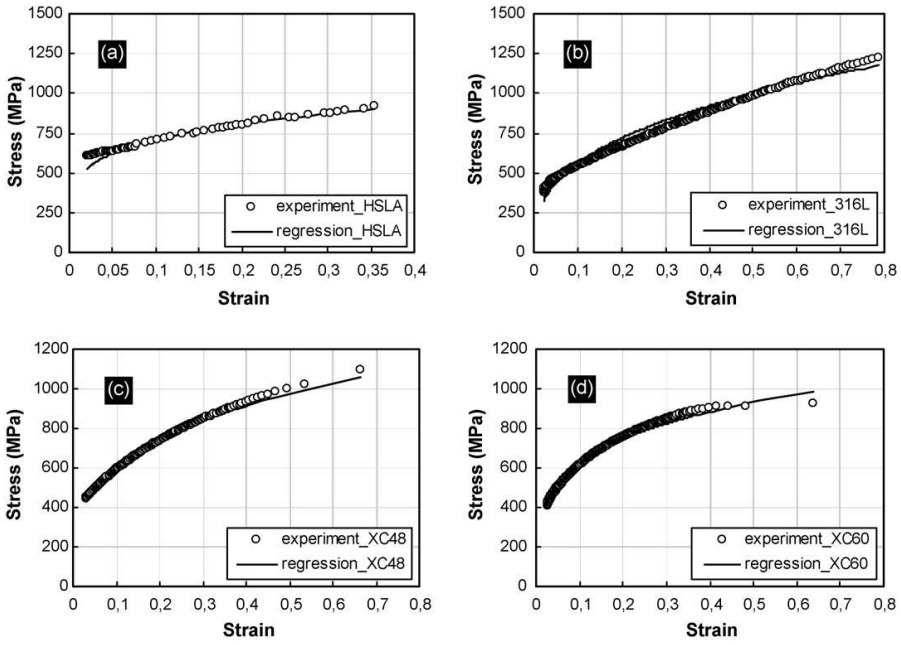

Figure 23. Stress-strain curves for steel alloys [48]

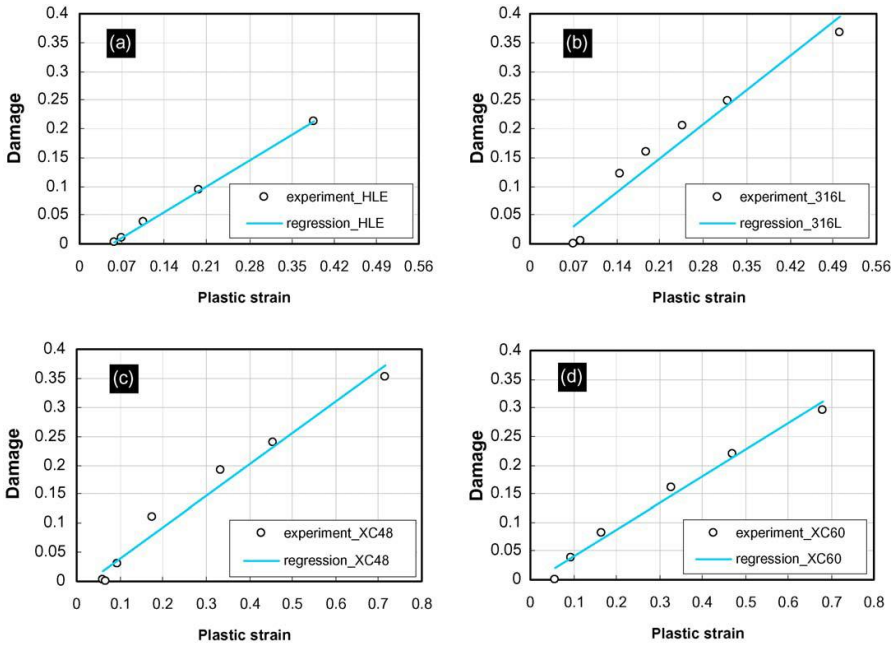

Figure 24. Identified damage using micro-hardness technique [48]

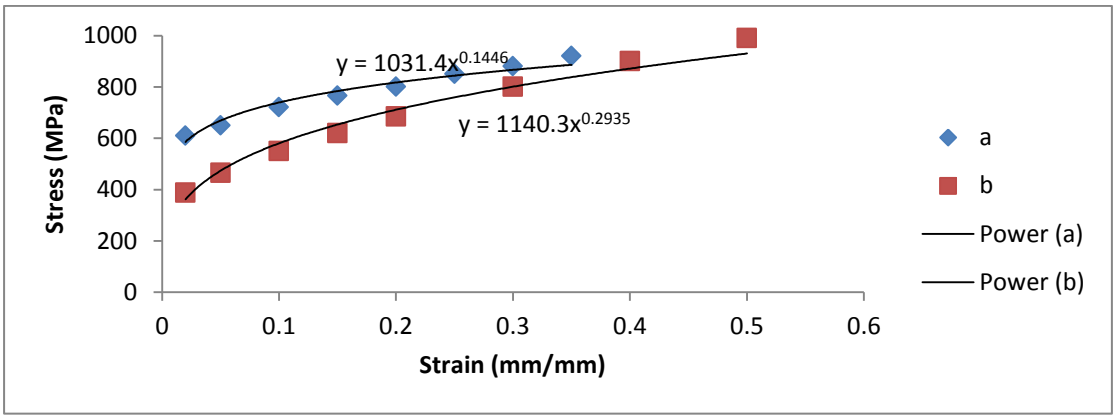

Figure 25. Hardening parameters for stress-Strain curves

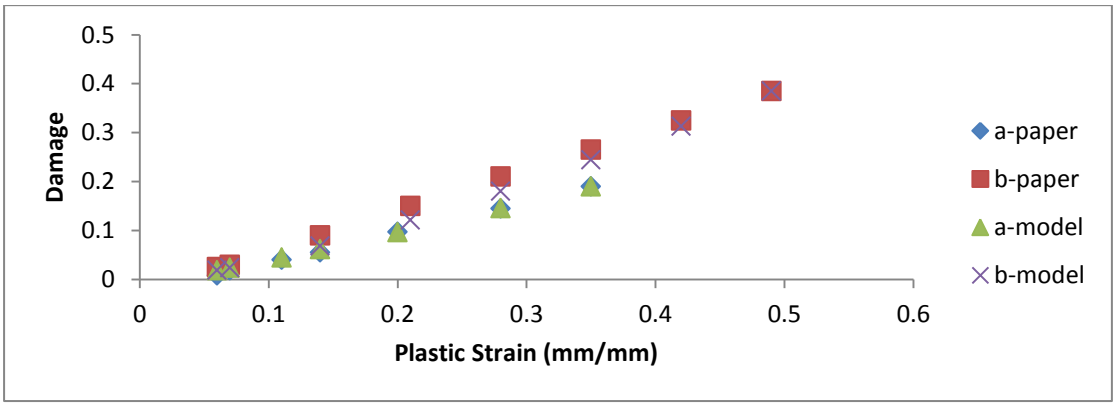

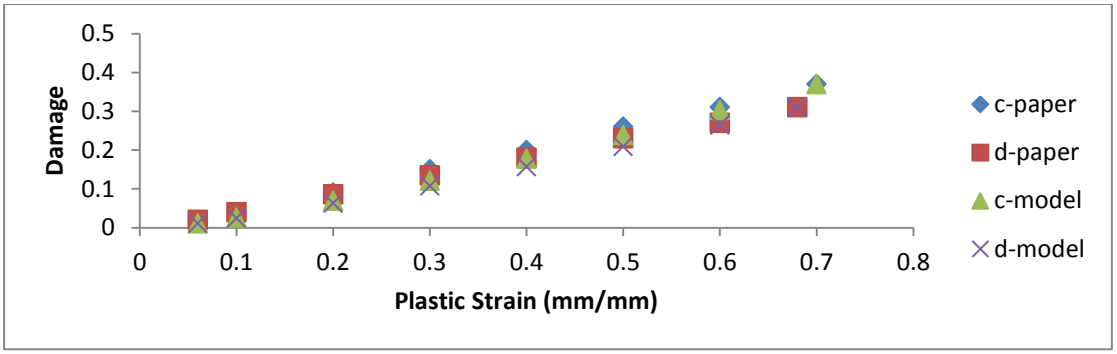

Figure 26. Comparison between literature results and the applied model

5.3.2.1.2 CASE 2: Experimental and Numerical Characterization of Damage Evolution in Steels [47]

This work performs experimental and numerical characterization of ductile damage in steels. The damage was evaluated using the loss of stiffness during the deformation process by carrying out tensile tests with loading-unloading cycles. The damage was assumed to be isotropic and to behave linearly with plastic strain. These two assumptions were set for simplicity reasons and as an initial study. Authors recommended through the paper suggestions of further work incorporating anisotropic damage and considering the damage exponent to be quadratic since damage is highly a non-linear process. The stress–strain curve of SAE 1020 steel along with the damage results are presented in Figure 27. Strain hardening parameters were obtained and the comparison between the proposed model and the published work is shown in Figure 28.

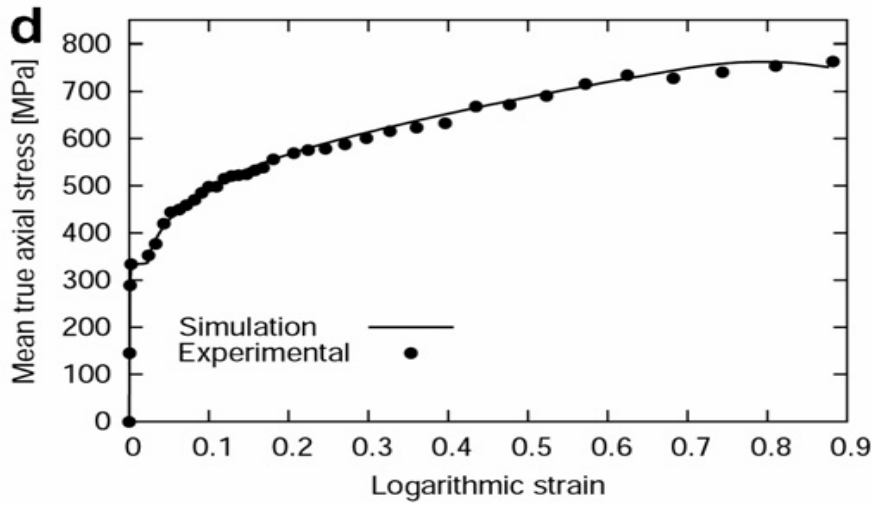

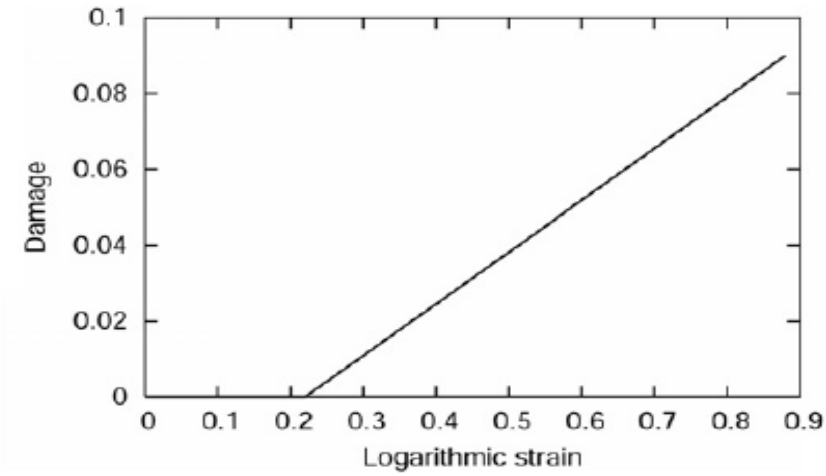

Figure 27. Stress-strain curve for SAE1020 steel and resulting damage relation [47]

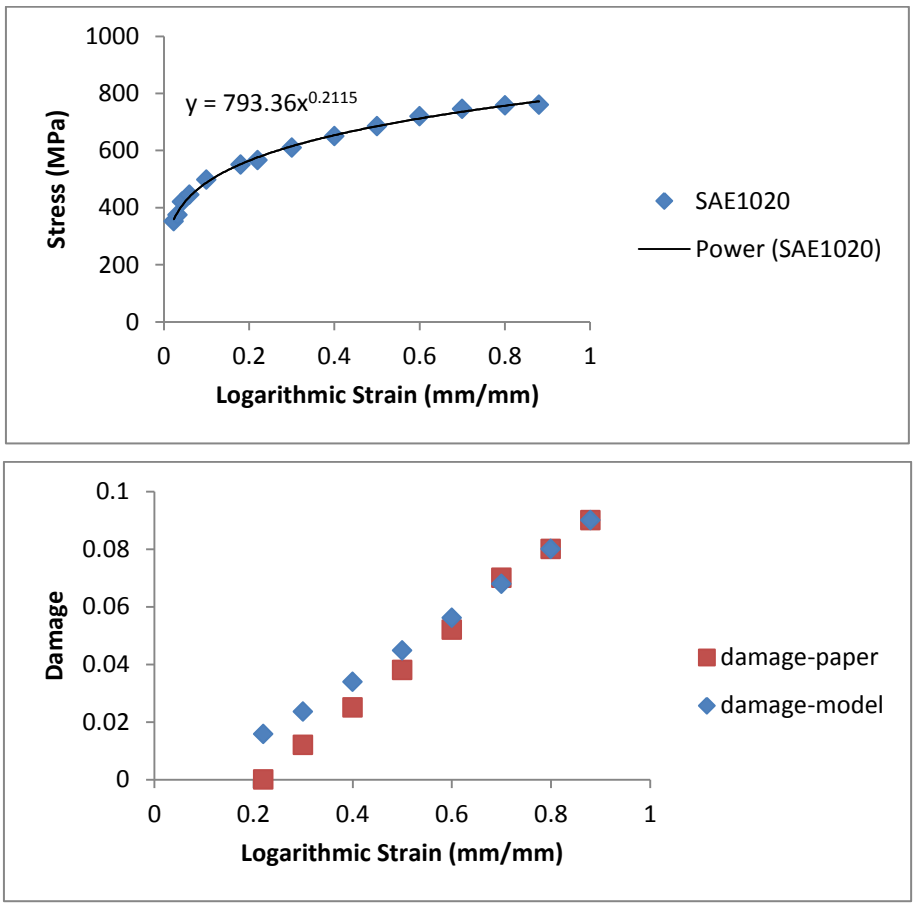

Figure 28. Material hardening parameters and comparison of damage between literature and proposed model

5.3.2.1.3 CASE 3: Identification and Measurement of Ductile Damage Parameters [8]

The damage parameters were found using continuum damage mechanics (CDM) approach by finding the reductions in Young's Modulus. The stress-strain curves indicated in the paper along with the constructed one in order to obtain the hardening parameters are presented in Figure 29. The damage exponent was used as 0.7. Comparisons between both damage values are displayed in Figure 30.

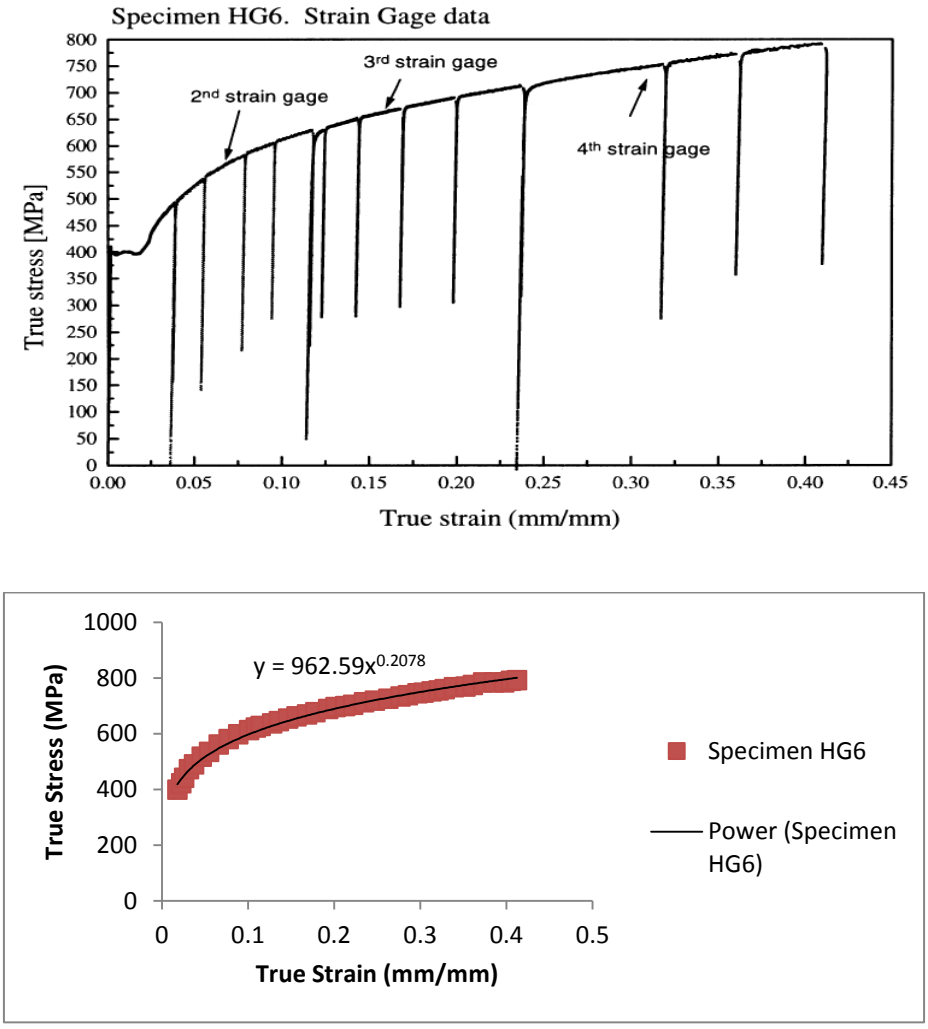

Figure 29. Stress-strain curves from the literature and reconstrucion with hardening parameters [8]

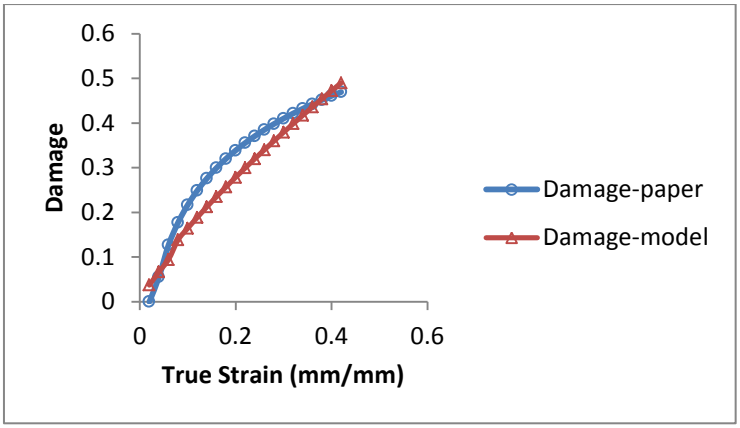

Figure 30. Damage from Bonora's work and proposed energy based model

5.3.2.2 Model Verification Using Finite Element Simulation

This section discusses in detail the modeling and results of the finite element simulations performed in ABAQUS software. Both the numerical procedure and identification of material parameters were verified on the basis of uniaxial tension test.

5.3.2.2.1 General Procedure

Crack and Void propagation in the structure is often simulated with finite element (FE) analysis based on continuum mechanics. There are four ways to simulate damage propagation in a finite element model; splitting of elements, nodes separation, decreasing elements stiffness and deleting damaged elements. In this research, the third technique has been used in order to evaluate the damage variable. The predicted responses have been calculated by employing the ABAQUS finite element code. This code provides a user subroutine, in which the model has been implemented. For each strain rate, the damage parameter for all the elements in the model was calculated on the basis of the energy model.

5.3.2.2.2 Input Variables

5.3.2.2.2.1 Material Description

The numerical prediction depends mainly on the correct description of the material behavior. Mechanical properties were obtained from the uniaxial tensile tests of steel. True stress-true strain curves were entered in the material description in

ABAQUS and the hardening behavior was mimicked using Johnson Cook (J-C) model; Eq. 17. The J-C model is used to accurately predict the response of a material with considering the strain rate effects on the flow stress. Furthermore, it is simple and intended mainly for use in computer codes.

$$\bar{\sigma} = [A + B(\bar{\varepsilon}^{pl})^n]\left[1 + C \ln\left(\frac{\dot{\bar{\varepsilon}}^{pl}}{\dot{\varepsilon}_o}\right)\right] \quad \text{Eq.17}$$

Where:

$\bar{\sigma}$ is the yield stress at nonzero strain rate;

A, B, C and n are material parameters

$\bar{\varepsilon}^{pl}$ is the equivalent plastic strain

$\dot{\bar{\varepsilon}}^{pl}$ and $\dot{\varepsilon}_o$ is the equivalent plastic strain rate

The J-C model constants A, B, C and n are determined from the experimental true stress- true strain results using a numerical technique. Table 3 shows the values for these parameters that were implemented in the finite element simulations. These parameters were able to model the hardening behavior at different strain rates as depicted in Figure 31 for the lowest and the highest strain rate.

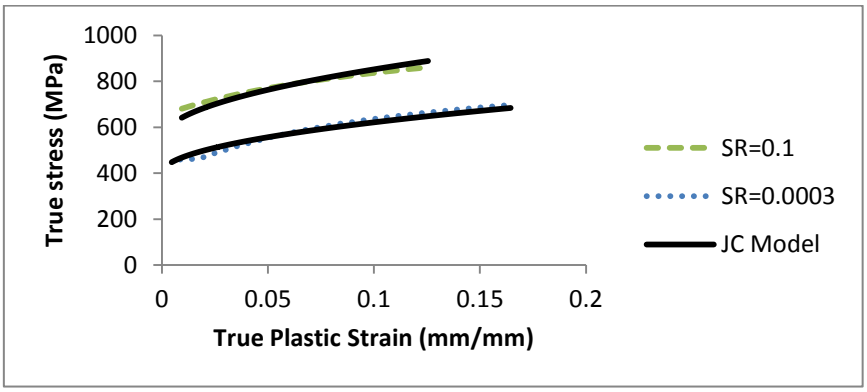

Figure 31. Example of correlation between experimental data and Johnson Cook model predictions

Table 3: Johnson Cook model parameters for the present steel

Parameter	A	B	C	n	$\dot{\varepsilon}_o$ (s^{-1})
Value	445	700	0.065	0.5	0.000333

5.3.2.2.2.2 Damage Initiation and Evolution

The strain threshold at which damage initiates is entered in ABAQUS as the start of the plastic strain. After damage initiation, the material stiffness is degraded progressively according to the specified damage evolution response. Damage evolution was defined as a function of the plastic displacement after damage initiation with maximum degradation option so that the current damage evolution mechanism will interact with other damage evolution mechanisms in a maximum sense to determine the total damage from multiple mechanisms. The initiation of a macro crack in the structure occurs at any point when the damage variable reaches its critical value, φ_c, a value at which ductile failure will occur. In our numerical analysis this value at any Gauss point was set to be 1. Once this value is reached the damaged elements are removed and the crack will advance.

5.3.2.2.3 FE Modeling

Symmetry conditions are imposed in order to model only one quarter of the geometry. Assuming axisymmetry for the cylindrical specimen, a quarter of the problem is discretized with a height of 12.5mm (half of the initial gage length) and a linear radius variation along the bar according to the geometry specifications. This requires that all nodes along the x=0 axis have their x-displacements constrained to zero; all nodes along the y=0 axis have zero y-displacement. Geometrical imperfection was used to force necking and localization in the center of the specimen.

The mesh is built up in order to describe correctly the large stress and deformation gradients expected in the necking zone. More elements are placed near the center of the specimen at x=0 and fewer at the end of the bar at x=100. A quarter numerical model consists of 686 4-node quadrilateral elements as shown in Figure 32.

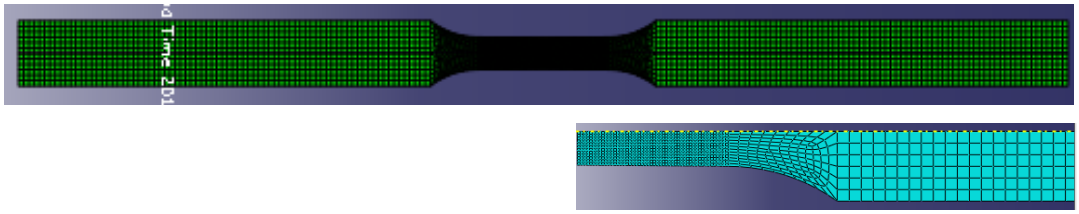

Figure 32. Modeled bar and one quarter of the cylindrical steel specimen

Mesh dependency was alleviated by applying several gradually finer meshes till the effects of mesh size were negligible. All simulations were conducted with imposed velocity on the lower and upper parts of the specimens.

5.3.2.2.4 FE Simulation Results

In order to test the implementation, the flow curve was determined first. The evaluation of the stresses and strains was done at the Gaussian points along the x=0 axis. The experimental values are represented accurately by these calculations; Figure 33. It can be seen from the contours in Figure 34 that the equivalent plastic strain is uniform along the smallest cross-section and the shear stresses at the neck are almost equal to zero.

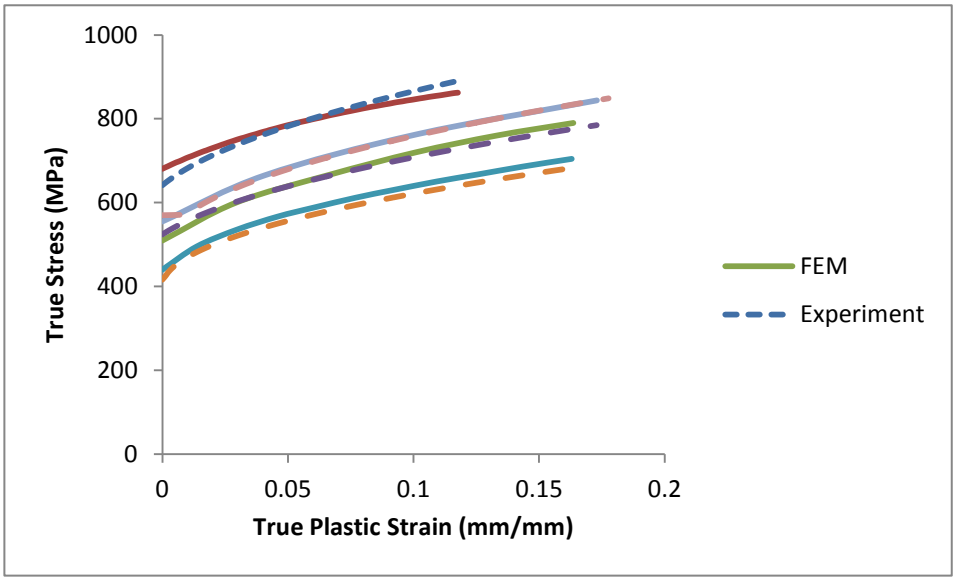

Figure 33. Flow curve from finite element simulations and experimental results

The model can detect the initiation time and location of damage. DUCTCRT output variable indicates that the damage initiation criterion has been met once its value is 1 or higher. The contours in Figure 35 show the damage initiation starting from the necking zone. After this stage, the damage evolution process is defined and the damage variables are obtained for different strain rates.

The finite element implementation of the proposed energy model is carried out resulting in the set of nodal displacements and nodal damage. Results are presented and discussed in terms of the effect of the strain rate on the damage level and the exponent of the damage evolution.

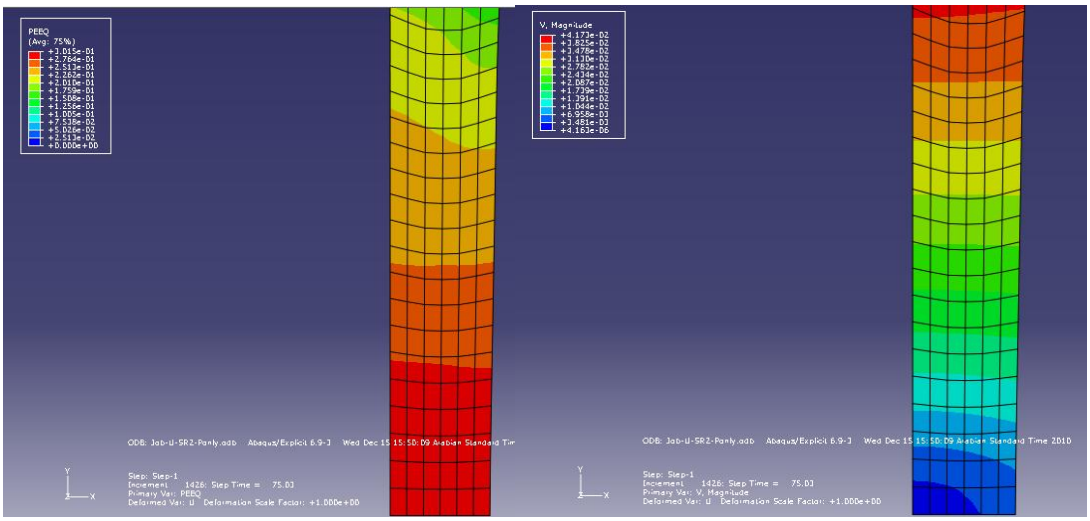

Figure 34. Enlarged views of the neck section with contours showing equivalent plastic strain and shear stresses

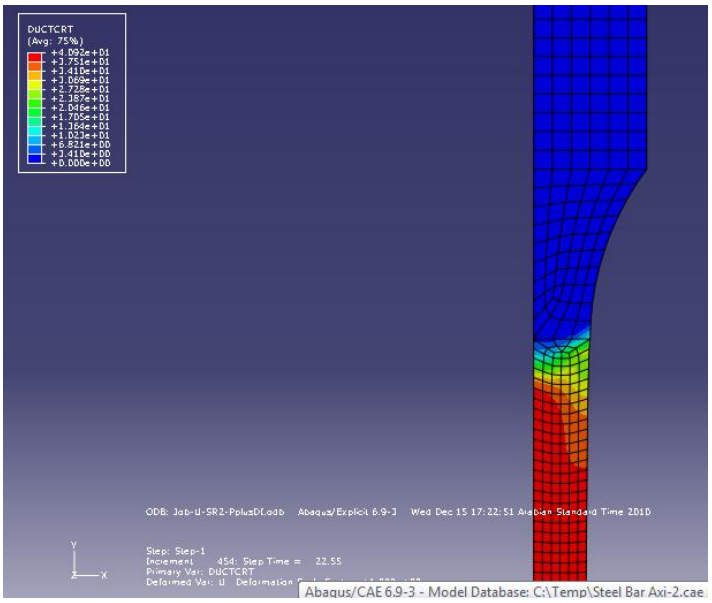

Figure 35. Damage initiation criterion

The maximum value of degradation was set to be 1. The output variable SDEG represents the value of the damage variable φ. The damage variables versus strain are presented in Figure 36. The results were comparable to the proposed model; Figure 37.

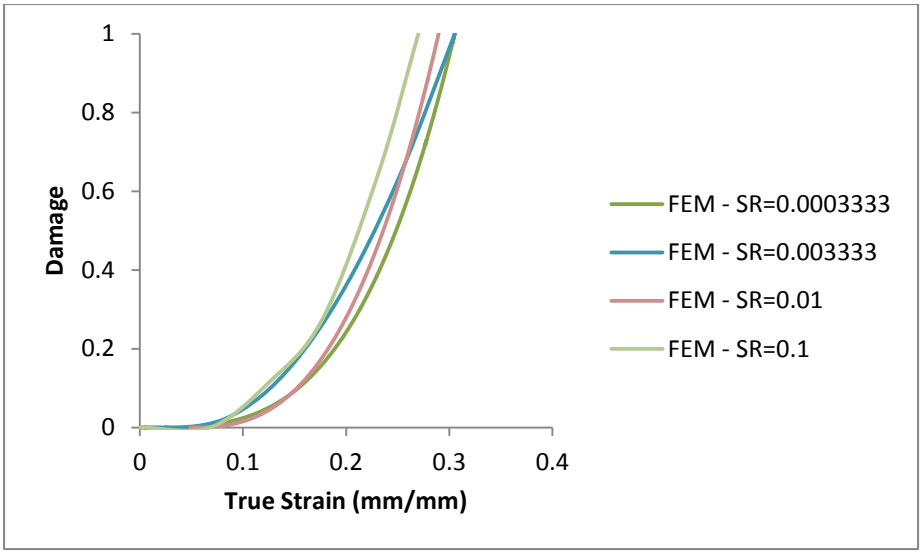

Figure 36. Damage vs. strain at different strain rates

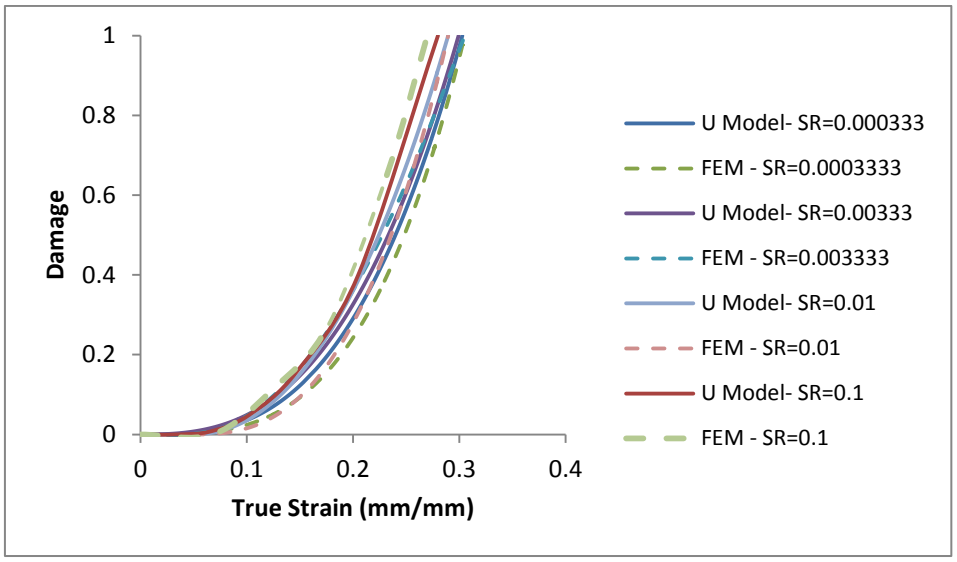

Figure 37.Verification of the energy based model using finite element analysis

CHAPTER 6

ANALYSIS AND DISCUSSION

In this chapter, results are compared and discussed in terms of the effect of the strain rate on the damage level and the differences in each approach.

6.1 Effect of Strain Rate on Damage

Generally for all approaches, the higher the strain rate, the higher the value of damage. Towards higher strain rates, the damage variable increases in a faster manner; Figure 38. It is obvious that the damage increases with the accumulation of strain. This suggests that, with increasing rate of loading, the steel is damaged more severely and pushed closer to a complete state of fracture.

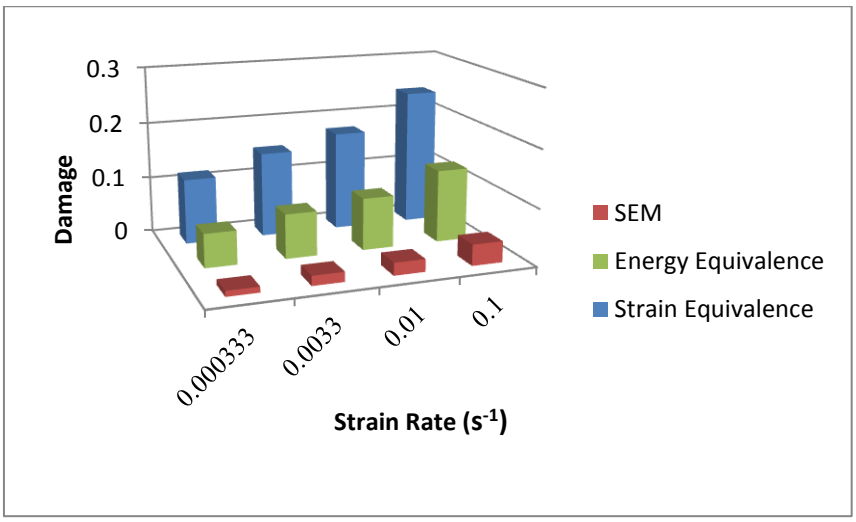

Figure 38. Difference in damage levels at different strains for various approaches

6.2 Comparison between Different Approaches

Even for a single material, the damage evolution parameters obtained with the different experimental methodologies will never be exactly equal, however, a detailed comparative analysis of the limitations and capabilities of these methodologies is lacking in the literature. Therefore, this work quantitatively compares three experimental damage quantification methodologies: damage area fraction by SEM, damage from loss of stiffness, and damage obtained from a new energy based model.

The comparison is based on the damage evolution up to the point of fracture in steel deformed in a uniaxial-tension strain path.

Furthermore, the results show that the damage variable increases nonlinearly with plastic strain. The final deformation phase prior to failure is dominated by the void coalescence process that rapidly pushes the net resisting area to instability. This probably can describe the nonlinearity of the damage model that is characterized by the damage exponent α that describes the kinetic law of damage evolution as a function of the accumulated plastic strain. The ductile damage process is highly nonlinear and there are no reasons why the dissipation should remain constant in each of the initiation and growth stages.

In order to properly investigate the agreement between theoretical and experimental results including the direct and indirect approaches, damage values were normalized to one damage value at failure for all strain rates. For the sake of comparing the damage values at failure, the results using the strain equivalence and energy equivalence were extrapolated to the failure strain, since it becomes difficult to measure the modulus of elasticity during unloading before failure, as pointed out previously in the literature review chapter.

It is very clear from Figures 39 and 40 that the assumption for the quadratic relation between strain and damage is valid for all approaches for the present research material. The proposed model predictions show very good correlations with the experimentally measured damage values at the four considered strain rates.

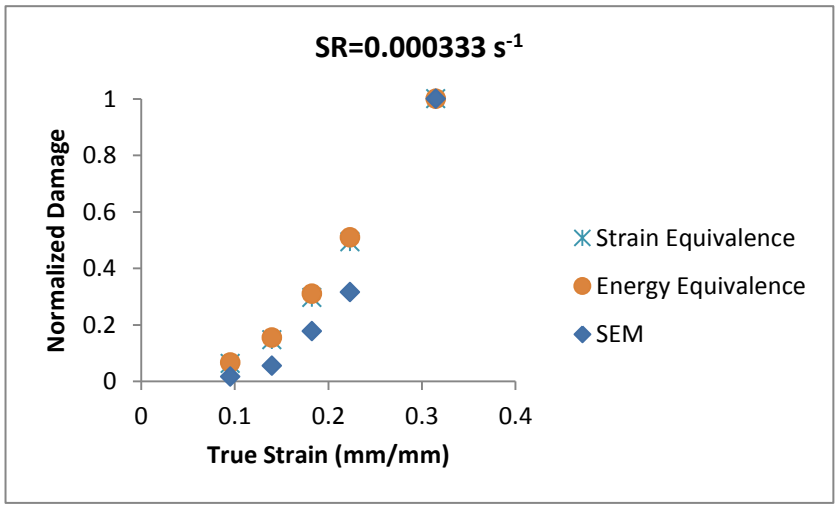

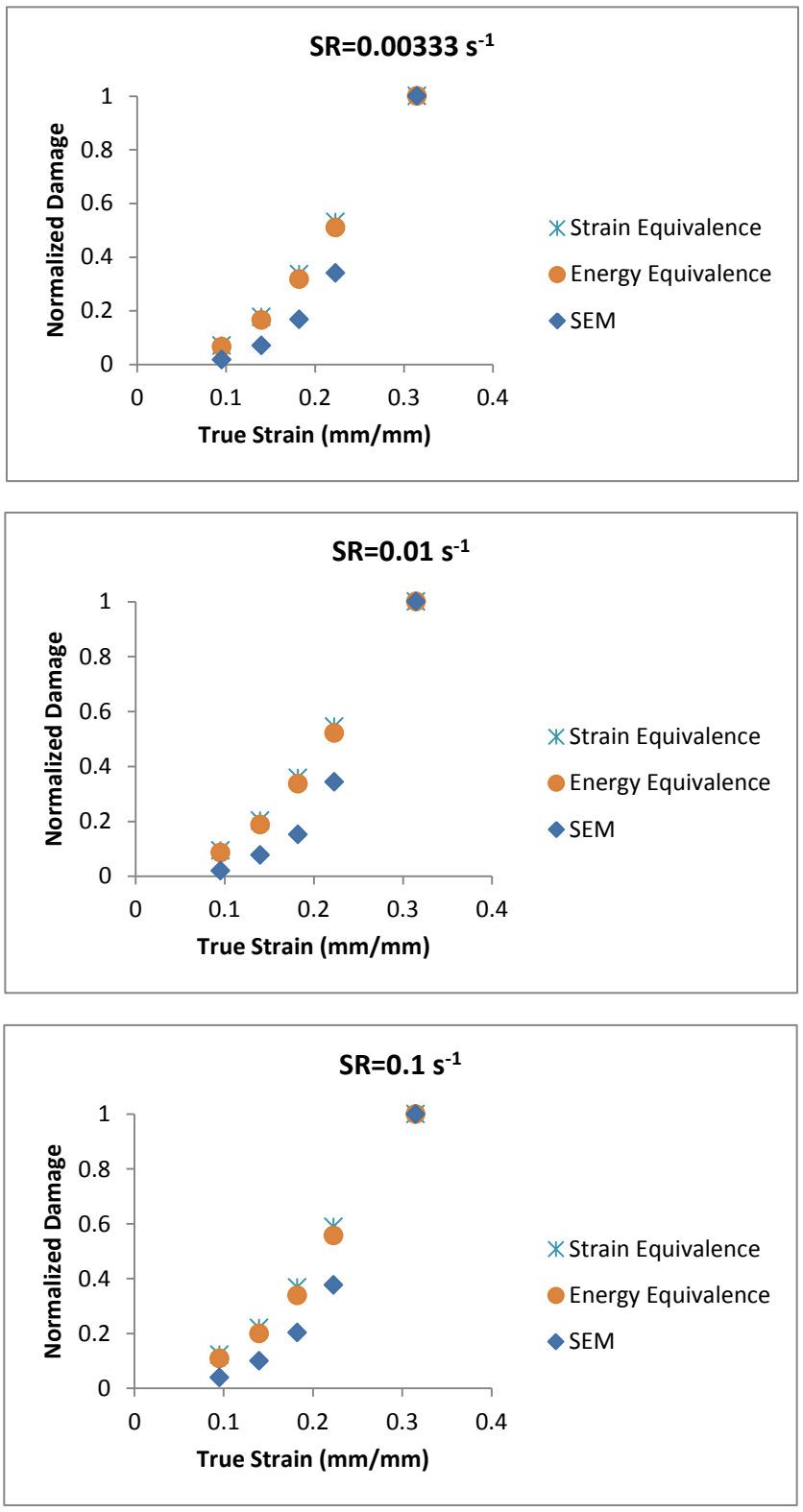

Figure 39. Normalized damage vs. true strain for reduction in Young's modulus and SEM results

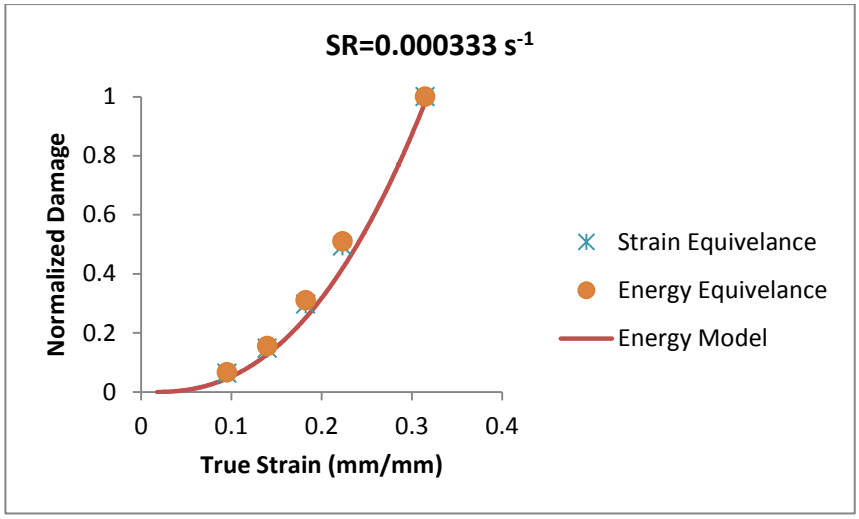
SR=0.000333 s-1
Normalized Damage
1
0.8
0.6
0.4
0.2
0
0
0.1
0.2
0.3
0.4
True Strain (mm/mm)
Strain Equivelance
Energy Equivelance
Energy Model

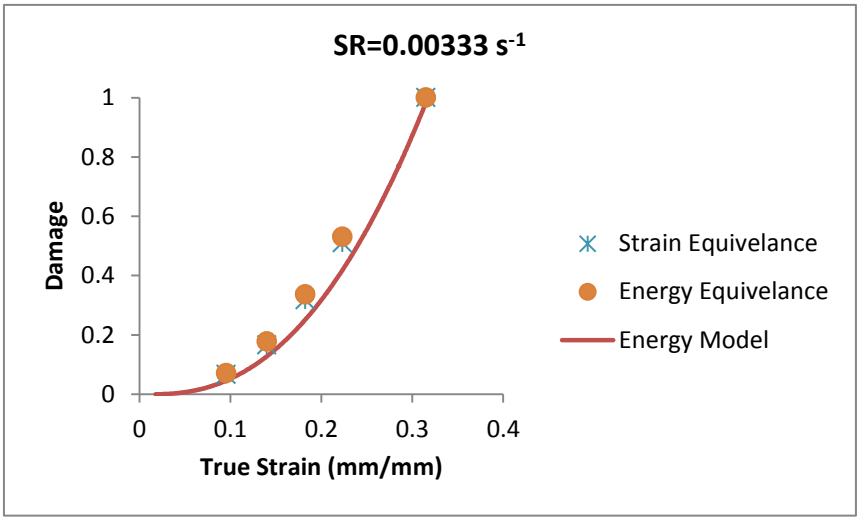
SR=0.00333 s-1
Damage
1
0.8
0.6
0.4
0.2
0
0
0.1
0.2
0.3
0.4
True Strain (mm/mm)
Strain Equivelance
Energy Equivelance
Energy Model

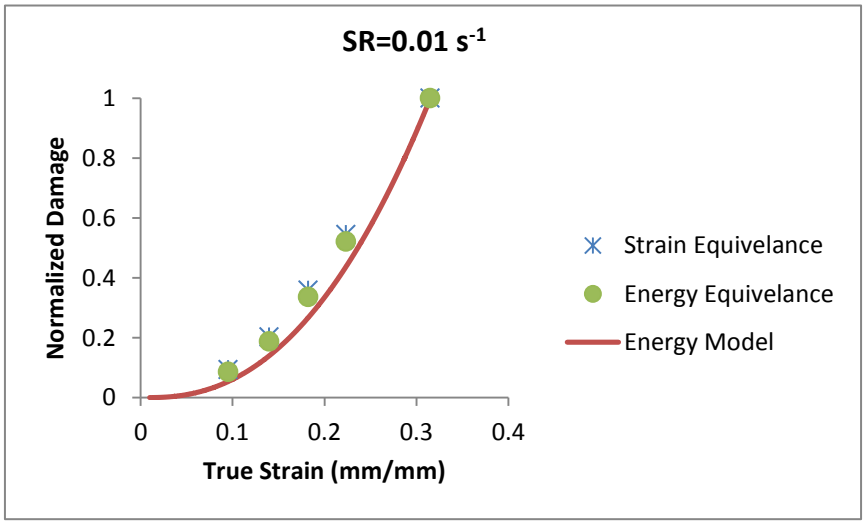
SR=0.01 s-1
Normalized Damage
1
0.8
0.6
0.4
0.2
0
0
0.1
0.2
0.3
0.4
True Strain (mm/mm)
Strain Equivelance
Energy Equivelance
Energy Model

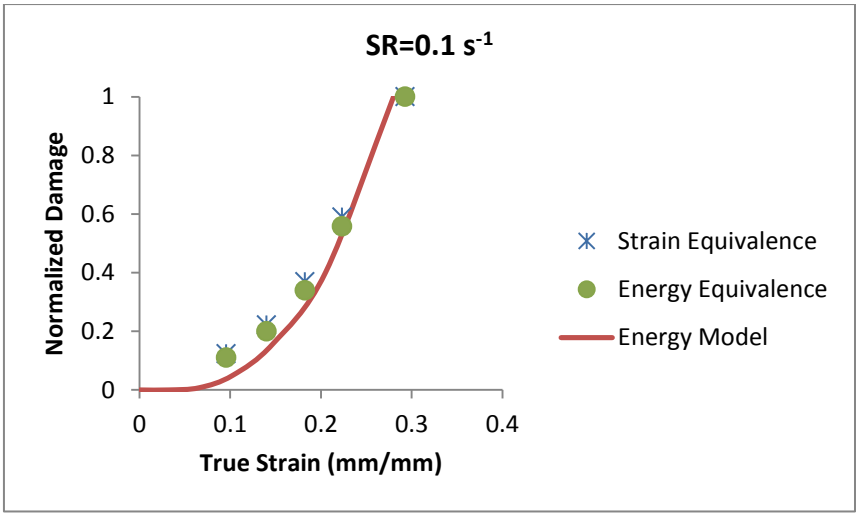

Figure 40. Comparison between reduction in Young's modulus and energy based model results

Comparisons between the measures damage values using SEM and the theoretically predicted results using the proposed energy model are also illustrated in Figure 41 at four different strain rates. The proposed damage model successfully predicted the experimental results in most cases.

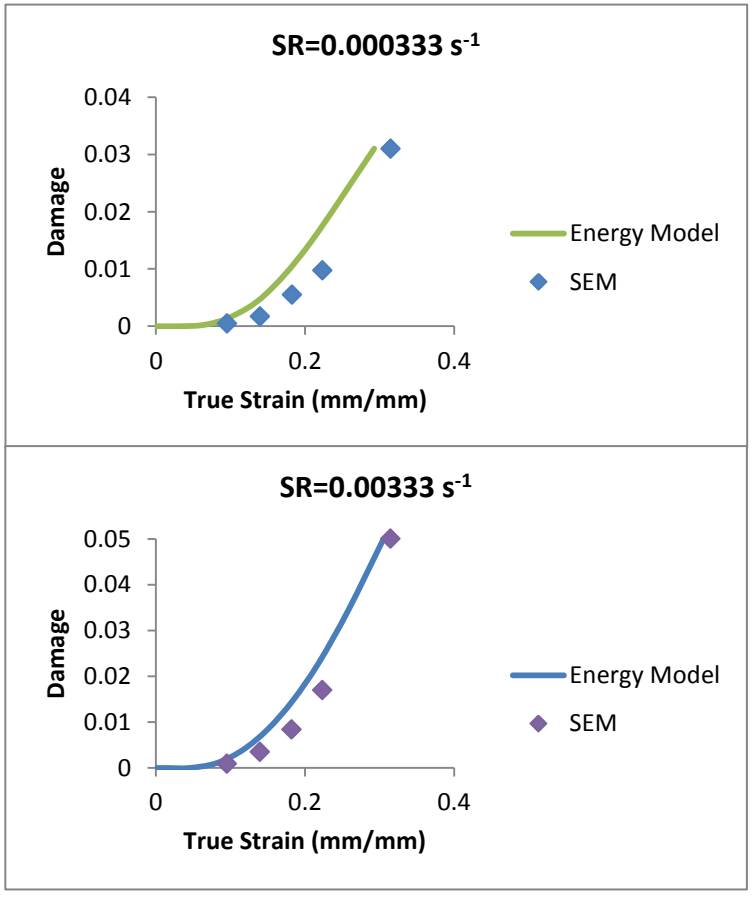

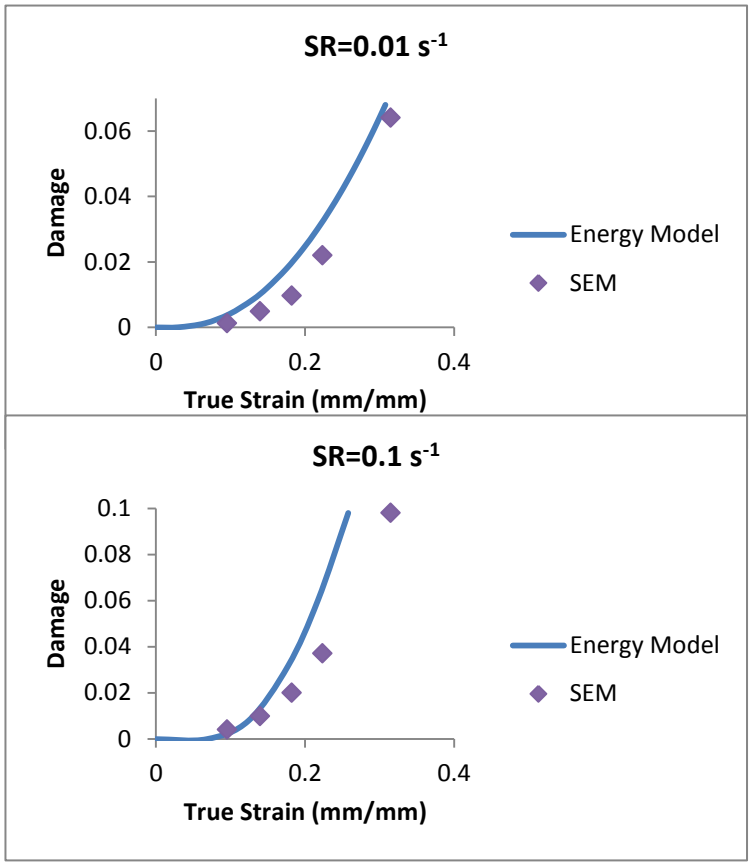

Figure 41. Comparison between SEM and energy model results (φ_f scaled to SEM φ_f)

It can be seen that the damage parameter depends on the definition and on the utilized experimental technique and therefore it can be considered as an adjustable parameter as pointed out in the literature. Nevertheless, different damage values for the same material do not mean that they cannot be used as a material constant since the values are associated with different properties. In fact, choice of the most appropriate damage parameter is not an easy task and it is difficult to accommodate the various damage parameters shown in Table 4. Although the damage values using the elastic modulus change and the damage using SEM theoretically ought to be the same since they share the same basic definition of Eq.1, the actual experimental data show they are not. The damage obtained from SEM is much smaller than the ones obtained using other approaches. In spite of the fact that the damage found from the decrease of the elastic modulus is related indirectly to the original damage concept of the formation of voids in a material during loading, it gave reasonable results compared to the finite element simulations and to the proposed energy model.

Table 4: Critical damage parameters for steel according to different definitions and experimental techniques

Damage Definition Method	Critical Damage Value at Strain Rate of (s^{-1})			
	0.000333	0.00333	0.01	0.1
Measurement of elastic modulus (Strain Equivalence)	0.22	0.28	0.32	0.41
Measurement of elastic modulus (Energy Equivalence)	0.12	0.153	0.176	0.23
Measurement of the voids area	0.031	0.050	0.064	0.098

The present data suggests that the hypothesis of energy equivalence is more appropriate than the strain equivalence since it gives smaller values of damage that are closer to SEM measurements. This cannot be considered as a general finding since only one material was tested. Table 5 lists some of the damage data reported in the literature for different materials. It is evident that the damage obtained from SEM measurements tends to be quite low, which is consistent with the present data. This definitely does not alleviate the fact that some errors are introduced with void measurement due to specimen preparation, image analysis and magnification, and instrumental errors.

Finally, the results showed that the proposed formula not only has the capability of predicting the damage effect correctly, but it can also be applied very conveniently in engineering practice by two-stage tests. Technically, it has to note that the proposed method is very easy to perform at less cost than the loading-unloading tests and the void measurements. Additionally, it can be said that the reliability of the method is acceptable.

Table 5: Critical damage values for different steels at room temperature and tested under strain rate=0.1 s^{-1} from the loss of stiffness: strain equivalence ($\varphi_f^{E\varepsilon}$) and energy equivalence (φ_f^{Eu}) and SEM measurements (φ_f^{SEM})

Material	φ_f^{SEM}	$\varphi_f^{E\varepsilon}$	φ_f^{Eu}	Ref.
Plain carbon steel 1045	0.035			[62]
Plain Carbon steel 1045	0.066			[59]
Plain Carbon steel 1090	0.048			[59]
Plain Carbon steel 1015	0.048			[59]
Mild Steel	0.006			[63]
SM41A structural steel	0.025			[64]
HSLA steel	0.100			[5]
HSLA Steel		0.205	0.108	[48]
XC60 Steel		0.37	0.206	[48]
Low alloy steel 20MnMoNi55		0.35	0.194	[65]
Steel AISI1010		0.2	0.105	[60]
Stainless Steel AISOS316		0.150	0.078	[60]
A533-B1 alloy steel		0.429	0.244	[17]

CHAPTER 7

CONCLUDING REMARKS

7.1 Summary and Conclusions

The term damage is used to indicate the deterioration of the material capability to carry loads. From a general point of view, damage develops in the material microstructure when nonreversible phenomena such as micro-cracking and micro-void formation take place. In this research, uniaxial tensile tests for steel bars were performed at four different strain rates. The tests were conducted to study damage accumulation and to develop a new theoretical model capable to predict damage at different strain rates. Loading-unloading were also carried out to determine the loss of stiffness at different stages in the deformation process. A representative element was cut from each specimen then utilized to quantify the voids fraction using the scanning electron microscope (SEM) device. A new energy-based damage model that has incorporated the damage potential as a dissipated energy was developed. The proposed damage model was successfully compared not only with the present experimental work but also with previous publications. Moreover, the predicted results were verified using finite element simulations conducted using the commercial software ABAQUS 6.9.3 explicit code.

A quantitative analysis of all approaches was presented. In all cases, an increase in damage was observed with increasing strain rates. Based on the experimental results including direct (SEM) and indirect (loading-unloading tensile tests) and the new developed energy model results, the following conclusions can be drawn:

- Towards higher strain rates, the damage has increased in a faster manner indicating the steel has been damaged more severely and pushed closer to a complete state of fracture.
- The comparisons have indicated a good agreement between the simulated and the applied energy model results.

- The energy model has proved its ability to capture the evolution of ductile damage as a function of strain in steel using finite element analysis and previous research data.
- The results using Scanning Electron Microscope gave much smaller values than the ones obtained using other approaches and this was found to be consistent with the literature.
- It has been seen from comparison between analyses and experiments as a function of strain rate that the stress-strain curves computed by FE analysis are good agreement with the experiments for all range of strain rate within ultimate elongation. It is therefore concluded that a FE analysis using a formulated strain rate-dependent model can be accurately predict the strain-rate dependent mechanical behavior of steel.

An effort was made to keep the newly developed energy model as simple as possible but still correctly represent the behavior of the structure. This work reflects the belief that only simple but effective models can gain some acceptance among practitioners.

7.2 Limitations and Future Research

Many problems were encountered during this research; below is a list of the main limitations faced:

- The absence of a specialized person in scanning electron microscope along with the delay in maintenance.
- The Instron machine has a limited range of strain rates.

In addition, suggestions for further work to extend this research and confirm its outcomes include:

- Examining more experimental techniques, e.g. variation of electrical resistance or ultrasonic test method for the determination of the damage variable.
- Assuring the geometry transferability of the damage parameters.
- Applying the newly presented model here to different metals and probably different materials such as composites.
- Utilizing the proposed technique to predict the effect of cycling.

- Considering temperature effects.
- Extending the study to much higher strain rates.
- Develop an implicit code in finite element software that incorporates the new proposed technique.

The implementation of the energy model for material characterization opens some questions that need to be answered in next researches:

Is this energy model applicable for metals or maybe other materials? Can it predict the effects of different loading regimes? And finally can this energy model be developed into an incorporated tool in finite element software?

REFERENCES

[1] N. Maeda, "Fundamental study on applications of damage mechanics to evaluation of material degradation," Nucl. Eng. Des., vol. 167, pp. 69-76, 1996.

[2] S. Winkler *et al.*, "Strain rate and temperature effects on the formability and damage of high strength steels," Metall. Mater. Trans., vol. 39, pp. 1350-1358, 2008.

[3] D. Steglich, "Micromechanical modelling of cyclic plasticity incorporating damage," Int. J. Solids Struct., vol. 42, pp. 337–351, 2005.

[4] G.Z. Voyiadjis and P.I. Kattan, *Advances in Damage Mechanics: Metals and Metal Matrix Composites*. Oxford: Elsevier, 1999, pp. 1-21.

[5] J. Lemaitre and J. Dufailly, "Damage measurements," Eng. Fract. Mech., vol. 28, no. 5-6, pp. 643-661, 1987.

[6] D. Krajcinovic, "Damage mechanics," Mech. Mater., vol. 8, no. 2-3, 1989, pp. 117–197.

[7] S. Baste and B. Audoin, "On internal variables in anisotropic damage," Mech. Mater., vol. 10, pp.587-606, 1991.

[8] N. Bonora, "Identification and measurement of ductile damage parameters," J. Strain Anal., vol. 34, no. 6, 1999, pp.463-478.

[9] B. F. Dyson *et al., Materials Metrology and Standards for Structural Performance*. London: Chapman and Hall, 1995, pp. 210-218.

[10] H. Stumpf and J. Saczuk, "On a general concept for the analysis of crack growth and material damage," Int. J. Plasticity, vol. 17, pp. 991–1028, 2001.

[11] J. Lemaitre and R. Desmorat, *Engineering Damage Mechanics: Ductile, Creep, Fatigue and Brittle Failures*. Netherlands: Springer, 2005, pp. 1-7.

[12] J.L. Chaboche, "Thermodynamics of local state: overall aspects and micromechanics based constitutive relations," Technische Mechanik, Band 23 Heft 2-4, pp. 113-119, June 2003.

[13] J.L. Chaboche, Continuum damage mechanics, Part I: General concepts, J. Appl. Mech., vol. 55, 1988, pp. 59-64.

[14] J. Lemaitre and J.L. Chaboche, *Mechanics of solid materials*. Cambridge: Cambridge University Press, 1990, pp. 346-449.

[15] *Ductile Fracture* [Online], Available: http://upload.wikimedia.org/wikipedia/ en/8/ 87/Ductile_fracture.PNG

[16] J. Lemaitre, “How to use damage mechanics,” Nucl. Eng. Des., vol. 80, 1984, pp. 233-245.

[17] M. Mashayekhi *et al.,* “Ductile crack growth based on damage criterion: Experimental and numerical studies,” Mech. Mater., vol. 39, 2007, pp. 623–636.

[18] L.M. Kachanov, “On the time to rupture under creep conditions,” Isv. Akad. Nauk. SSR. Otd Tekh. Nauk., vol.8, 1958, pp. 26-31.

[19] H. W. Tai, “Plastic damage and ductile fracture in mild steels,” Eng. Fract. Mech., vol. 36, no. 4, 1990, pp. 853-880.

[20] S. Chandrakanth and P. C. Pandey, “A new ductile damage evolution model,” Int. J. Fract., vol. 60, 1993, pp.73-76.

[21] N. Bonora, “A non-linear CDM model for ductile fracture,” Eng. Fract. Mech., vol. 58, no. 1-2, 1997, pp. 11-28.

[22] M. Zheng *et al.*, “Ductile Damage Model Corresponding To the Dissipation of Ductility of Metal,” Eng. Fract. Mech., vol. 53, no. 4, 1996, pp. 653-659.

[23] N. Bonora *et al.,* “Identification of the parameters of a non-linear continuum damage mechanics model for ductile failure in metals,” J. Strain Anal. Eng. Des., vol. 39, 2004, pp. 639–651.

[24] H. LaEmmera and Ch. Tsakmakisa, “Discussion of coupled elastoplasticity and damage constitutive equations for small and finite deformations,” Int. J. Plasticity, vol. 16, no. 5, 2000, pp. 495-523.

[25] V.A. Lubarda and D. Krajcinovic, “Some fundamental issues in rate theory of damage-elastoplasticity,” Int. J. Plasticity, vol. 11, 1995, pp.763-797.

[26] S. Dhar *et al.,* “A continuum damage mechanics model for void growth and micro crack initiation,” Eng. Fract. Mech., vol. 53, 1996, pp. 917-928.

[27] R.D. Thomson, J.W. Hancock, “Ductile failure by void nucleation, growth and coalescence,” Int. J. Fract., vol. 26, 1984, pp. 99–112.

[28] J. Lin *et al.,* “A review on damage mechanics, models and calibration methods under various deformation conditions,” Int. J. Damage Mech., vol. 14, 2005, pp. 299–319.

[29] J.L. Chaboche, “Anisotropic creep damage in the framework of continuum damage mechanics,” Nucl. Eng. Des., vol. 79, 1984, pp. 309-319.

[30] S. Murakami, “Anisotropic aspects of material damage and application of continuum damage mechanics,” in *CISM Courses and Lectures No. 295,*D. Krajcinovic and J. Lemaitre, Eds., Wien, Springer, 1987, pp. 91-133.

[31] J.P. Cordebois and F. Sidoroff, “Damage Induced Elastic Anisotropy,” in *Mechanical Behaviour of Anisotropic Solids*, J.P. Boehler, Ed., London, Martinus Nijhoff, 1979, pp. 761–774.

[32] F. Sidoroff, “Description of anisotropic damage application to elasticity,” in IUTAM colloquim on physical nonlinearities in structural analysis, Berlin, Springer-Verlag, 1981, pp. 237-244

[33] A. Cauvin and R.B. Testa, “Elastoplastic material with isotropic damage,” Int. J. Solids Struct., vol. 36, no. 5, 1999, pp. 727-746.

[34] R.K. Abu Al-Rub and G.Z. Voyiadjis, “On the coupling of anisotropic damage and plasticity models for ductile materials,” Int. J. Solids Struct., vol. 40, no. 11, 2003, pp. 2611- 2643.

[35] L.M. Kachanov, *Introduction to continuum damage mechanics*. Netherlands: Kluwer Academic Publishers, 1986, pp. 51-62.

[36] C.L. Chow and L.G. Yu, “A unified approach to metal fatigue based on the theory of damage mechanics,” in *Applications of continuum damage mechanics to fatigue & fracture, ASTM STP 1315*, D.L. McDowell, Ed., American Society for Testing and Materials,1997, pp. 165-185.

[37] D. Gross and T. Seelig, *Fracture Mechanics with an Introduction to Micromechanics*. Berlin: Springer, 2006, pp. 289-300.

[38] N. Bonora *et al.,* “Crack initiation in A1-Li alloy using continuum damage mechanics,” in *Localized Damage Ili Computer-Aided Assessment and Control,* M. H. Aliabadi *et al.*,Eds., Southampton: Computational Mechanics Publication, 1994, pp. 657-665.

[39] Y.S. Cheng and Y. Huang**,** “Measurement of continuous damage parameter,” Eng. Fract. Mech., vol. 31, no. 6, 1988, pp. 985-992.

[40] L.B. Wang *et al.,* “Quantification of damage parameters using X-ray tomography images,” Mech. Mater., vol. 35, 2003, pp. 777–790.

[41] J.L. Chaboche, “Continuum damage mechanics, Part II: Damage growth crack initiation and crack growth,” J. Appl. Mech., vol. 55, 1988, pp. 65-72.

[42] A. El Bartali *et al.*, “Surface observation and measurement techniques to study the fatigue damage micromechanisms in a duplex stainless steel,” Int. J. Fatigue, vol.31, 2009, pp.2 049–2055.

[43] D. Chae and D. A. Koss, “Damage accumulation and failure of HSLA-100 steel,” Mater. Sci. Eng., vol. 366, no. 2, 2004, pp. 299-309.

[44] S. Jansson and U. Stigh, “Influence of cavity shape on damage parameter,” J. Appl. Mech., vol.52, 1985, pp. 609–614.

[45] M. Garajeu *et al.*, “A micromechanical approach of damage in viscoplastic materials by evolution in size, shape and distribution of voids,” Comput. Methods in Appl. Mech. Eng., vol. 183, no. 3-4, 2000, pp. 223-246.

[46] C.C. Tasan *et al.*, “A critical assessment of indentation-based ductile damage quantification,” Acta Mater., vol. 57, 2009, pp. 4957–4966.

[47] D. J. Celentano and J.L. Chaboche, “Experimental and numerical characterization of damage evolution in steels,” Int. J. Plasticity, vol. 23, 2007, pp. 1739-1762.

[48] A. Mkaddema *et al.*, “A new procedure using the micro-hardness technique for sheet material damage characterization,” J. Mater. Process. Technol., vol. 178, 2006, pp. 111–118.

[49] G. Arnold *et al.*, “Identification of continuum damage model from microhardness measurements,” Pred. Defects Mater. Process., vol. 5, 2002, pp. 10–21.

[50] G. Baudin, H. Policella, “Novel method of measuring crack length using electric potential,” (in French), Recherche Ae´rospatiale, vol.4, 1978, pp. 195–203.

[51] G. Cailletaud *et al.*, “Effect of damage on electrical resistance of metals,” (in French), C. R. Acad. Sci., vol. 92, no. 2, 1989, pp. 1103–1106.

[52] R. Caoa *et al.*, “Effects of loading rate on damage and fracture behavior of TiAl alloys,” Mater. Sci. Eng., vol. 465, 2007, pp. 183–193.

[53] F.L. Addessio and J.N. Johnson, “Rate-dependent ductile failure model,” J. App. Phys., vol.74, no.3, 1993, pp. 1640–1648.

[54] D. C. Brooker and B.F. Ronalds, “Prediction of ductile failure in tubular steel members using ABAQUS,” in *International Society on Offshore and Polar Engineering Conference*, vol. 4, Stavanger, Norway, 2001. p. 45–50.

[55] ASTM Standard Test Methods for Tension Testing of Metallic Materials, ASTM E 8 96a, 2005.

[56] N. Bonora *et al.*, “Ductile damage evolution under triaxial state of stress: theory and experiments,” Int. J. Plasticity, vol. 21, 2005, pp. 981–1007.

[57] Instron Bluehill Software Reference, Instron Inc., 2004.

[58] H. W. Tai, “Unified CDM model and local criterion for ductile fracture - I unified CDM model for ductile fracture,” Eng. Fract. Mech., 1992, vol. 42, no. 1, pp. 177-182.

[59] G. Le Roy *et al.*, “A model of ductile fracture based on the nucleation and growth of voids,”Acta Metall., 1981, vol. 29, pp. 1509-1522.

[60] J. Lemaitre, *A Course on Damage Mechanics.* 2nd ed., Berlin: Springer, 2006.

[61] D.C. Joy, “Scanning electron microscopy for materials characterization,” Current opinion in solid state and material science, vol. 2, 1997, pp.465-468.

[62] A. Brownrigg *et al.*, “The influence of hydrostatic pressure on the flow stress and ductility on a spherodized 1045 Steel,” Acta Metall., vol. 31, no. 8, 1983, pp.1141–1150.

[63] Z.J. Luo *et al.*, “A ductile damage model and its application to metal-forming processes,” J. Mater. Proc. Technol., vol. 30, 1992**,** pp. 31–43.

[64] A. Otsuka *et al.*, “Relationship between ductile crack initiation and void volume fraction,” Nucl. Eng. Des., vol. 105, 1987**,** pp.121–129.

[65] A. Pirondi *et al.*, “Simulation of failure under cyclic plastic loading by damage models,” Int. J. Plasticity, vol. 22, 2006, pp. 2146–2170.

APPENDIX

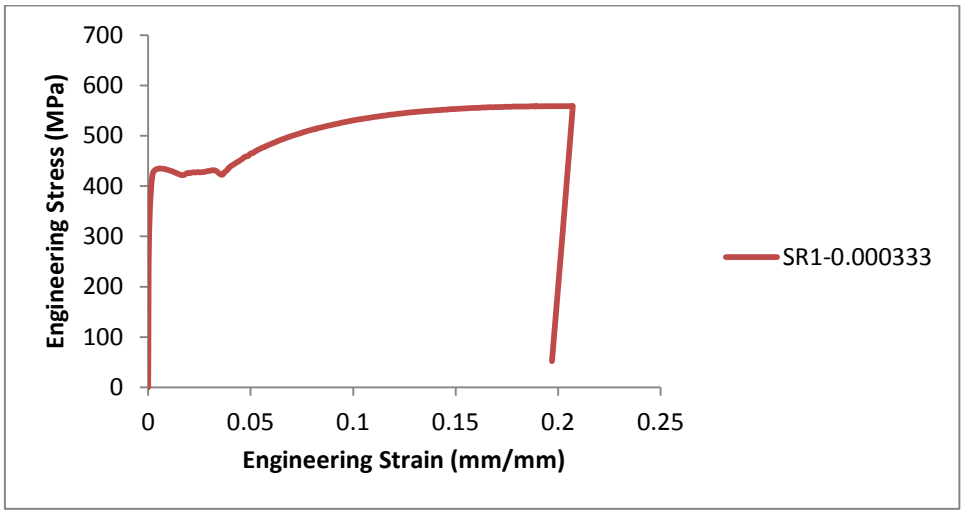
Engineering Stress (MPa)
700
600
500
400
300
200
100
0
0
0.05
0.1
0.15
0.2
0.25
Engineering Strain (mm/mm)
SR1-0.000333

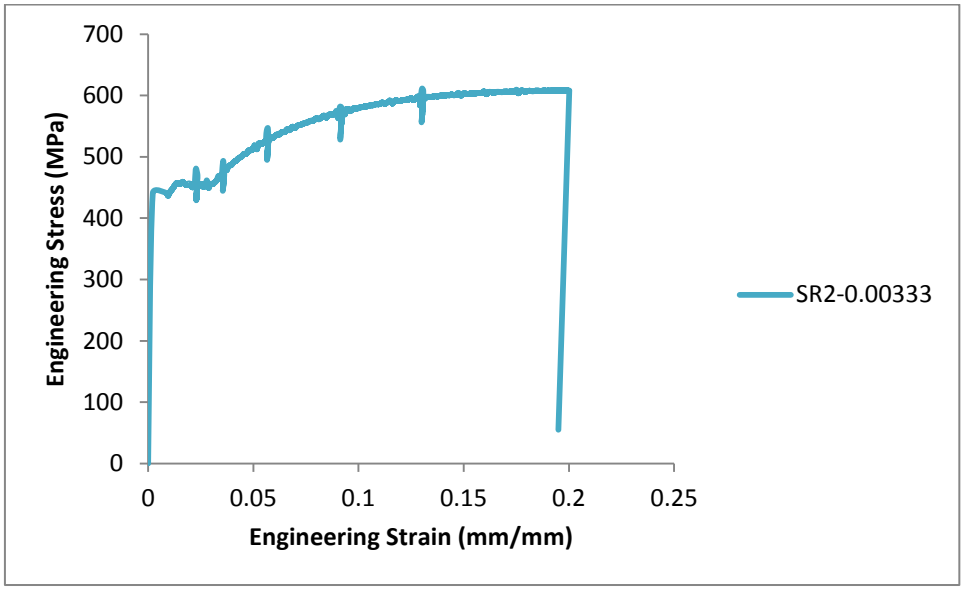
Engineering Stress (MPa)
700
600
500
400
300
200
100
0
0
0.05
0.1
0.15
0.2
0.25
Engineering Strain (mm/mm)
SR2-0.00333

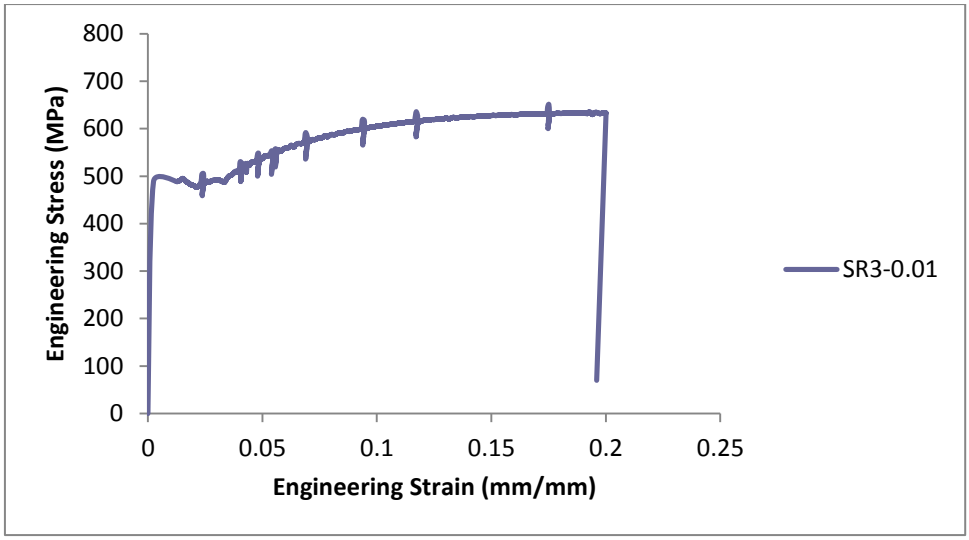
800
700
600
500
400
300
200
100
0
Engineering Stress (MPa)
0
0.05
0.1
0.15
0.2
0.25
Engineering Strain (mm/mm)
SR3-0.01

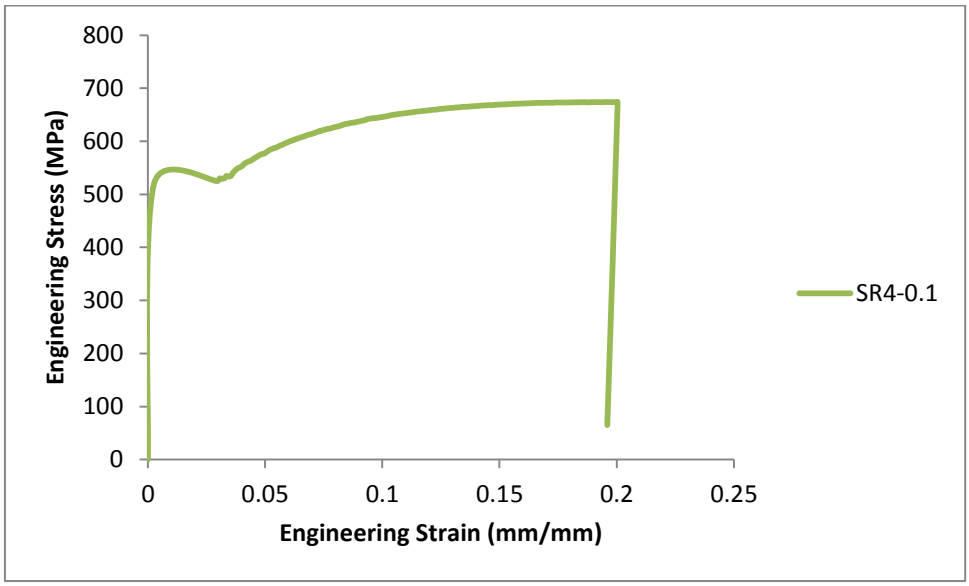
800
700
600
500
400
300
200
100
0
Engineering Stress (MPa)
0
0.05
0.1
0.15
0.2
0.25
Engineering Strain (mm/mm)
SR4-0.1

VITA

Reem Majeed Alhimairee was born on July 28, 1986, in Sharjah, UAE. She is from Iraq. She was educated in local public and private schools and graduated from Al-Gubaibah High School as tenth in class over UAE in 2004. She graduated from the American University of Sharjah earning a degree of a Bachelor of Science in Civil Engineering as a cum laude honor in 2009.

Ms. Reem worked as a Graduate Teaching Assistant at the American University of Sharjah while attaining her master's degree in Civil Engineering at the American University of Sharjah. She was awarded the Master of Science degree in Civil Engineering in 2011.

Ms. Reem is a member of the Institute of Structural Engineers, American Society of Civil Engineers, and the Engineering Women Society.